

Node-level community detection within edge exchangeable models for interaction processes

Zhang, Yuhua Dempsey, Walter
zyuhua@umich.edu wdem@umich.edu

Abstract

Scientists are increasingly interested in discovering community structure from modern relational data arising on large-scale social networks. While many methods have been proposed for learning community structure, few account for the fact that these modern networks arise from processes of interactions in the population. We introduce block edge exchangeable models (BEEM) for the study of interaction networks with latent node-level community structure. The block vertex components model (B-VCM) is derived as a canonical example. Several theoretical and practical advantages over traditional vertex-centric approaches are highlighted. In particular, BEEMs allow for sparse degree structure and power-law degree distributions within communities. Our theoretical analysis bounds the misspecification rate of block assignments, while supporting simulations show the properties of the network can be recovered. A computationally tractable Gibbs algorithm is derived. We demonstrate the proposed model using post-comment interaction data from Talklife, a large-scale online peer-to-peer support network, and contrast the learned communities from those using standard algorithms including spectral clustering and degree-correct stochastic block models.

Keywords— Large-scale Sparse Network, Edge Exchangeable Model, Community Detection, Interaction Process, Power-law Degree Distribution

1 Introduction

The WorldWideWeb, social media, and technological innovation allow people from around the world to easily interact across geographical, cultural and economic boundaries. Among its many benefits, increased connectivity enhances information flow, promotes community building, and facilitates the formation of support systems for individuals struggling with illness and addiction. In this paper, we focus on network data arising from sequences of interactions collected on social media platforms such as peer-to-peer support networks. Network data arising from such sequences naturally fit within models that treat the interaction as the statistical unit [5] rather than the users. Such networks often exhibit node-level community structure, i.e., an individual is more likely to comment on a post by someone from the same community.

Though there has been much progress on community detection, the current algorithms and models in the network literature do not account for the fact that many modern networks arise from processes of interactions. Edge exchangeable models [6] are built specifically to analyze datasets containing these complex interactions. Current models within the edge exchangeable framework can capture both global and local sparsity and power-law behavior [7]. While edge exchangeability is attractive as a theoretical framework, the set of current edge exchangeable models is inadequate to account for latent node-level communities which are common in modern network data.

Motivated by the important fact that most common complex networks constructed from interaction data exhibit latent node-level community behavior, we propose a new class of models in this paper, which extends the edge exchangeable framework to allow for community structure while permitting power-law degree and sparsity. Our main objective is the consistent identification of node-level latent communities as well as accurate estimates of the power-law parameters within each community.

1.1 Relevant Prior Work

A popular model class for community detection is the class of stochastic block models (SBMs) [14]. The simplest version of the SBM assumes vertices within the same block have the same probability of forming an edge (i.e., interact) with other vertices, and within-block interactions are more likely than between-block interactions. Many associated methods have been proposed. These include but are not limited to spectral clustering based methods ([22], [3]), Bayesian methods ([19], [17]), and pseudo-likelihood based methods ([2], [23]). The stochastic block model was later generalized to the degree-corrected stochastic block model (DC-SBM) [16], which allows for vertex degree heterogeneity. Theoretical guarantees of community recovery have been well established [11, 2, 32].

Prior literature has demonstrated empirical power law degree distribution in many communication and social networks [1]. That is, such networks contain a few high degree nodes and many low degree nodes. This network feature may be exploited when performing community detection. Recent work has extended the SBM to account for power-law degree distributions within each community [21]. Though SBM and the DC-SBM have been successfully applied in many situations, these approaches do not account for the fact that many modern networks arise from processes of interactions and are therefore ill-suited for network data arising in these settings. This is illustrated empirically via case study in Section 5.

1.2 Outline and main contributions

The main contributions of this paper are as follows:

1. We formally define network data with block structure and notation in Definition 2.2.
2. We define, in Section 2.4, the block vertex components models (B-VCM) - a subfamily of block edge exchangeable models that allow for node-level communities; we then prove a representation theorem for block edge exchangeable processes in Theorem 2.5.
3. We establish basic statistical properties of the B-VCM in Section 2.5. In particular, we

show the misspecification rate of block assignments can be bounded and the sparsity and power-law of the network can be guaranteed.

4. A computationally tractable Gibbs sampling inferential algorithm is derived in Section 3.2. Simulation results that support our models ability to capture power-law degree distributions and community structure are presented in Section 4.
5. We then apply our method to a peer-to-peer mental health support network in Section 5, contrasting the learned communities from those using standard algorithms including spectral clustering and degree-corrected stochastic block models.

We end the paper with a summary of the proposed methods and implications in Section 6. Overall this paper presents a statistically rigorous, principled framework for incorporating node-level communities into the edge exchangeability framework.

2 Block Edge Exchangeable Model

2.1 Motivating Example

Our motivating example is TalkLife, a large-scale online peer support network for mental health. Talklife’s users post short text snippets to which other users can react and/or comment. Each post consists of a poster and a set of commentators. Every post is flagged using machine-learning classifiers with at least one health-related topic, e.g, Anxiety/ Panic/ Fear suspected, Body Image/ Eating Disorders suspected and so on. The platform has collected millions of interactions among its users. A primary goal of TalkLife is to strengthen its peer support network and improve mental health outcomes for its users. A natural question that arises as part of this work is node-level community detection from the large-scale interaction data generated by the platform.

2.2 Notations and Data

We start by defining block structured interaction data. Inspired by the previous work on edge exchangeability [6], we extend the definition of interaction data to the setting where there exists an underlying block structure. To start, we consider a simple example based on interaction data from Talklife. Recall each TalkLife post consists of a poster s and a set of commentators $\{r_1, \dots, r_k\}$. Then a post on Talklife can be summarized by the ordered pair $\{\{s\}, \{r_1, \dots, r_k\}\}$. See Figure 1 for a visualization of Talklife’s interaction data and its corresponding network construction. Here, posters and commentators are drawn from the same underlying population, which we denote as \mathcal{P} . Definition 2.1 formalizes this example into a general definition of interaction data.

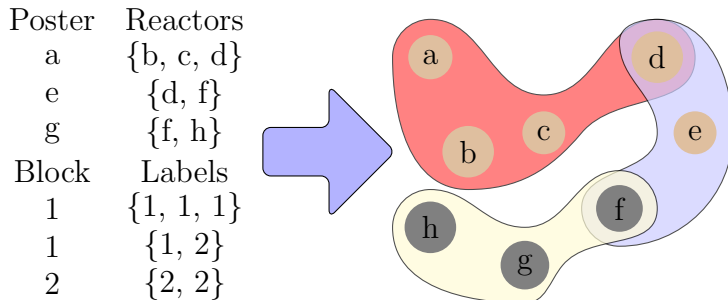


Figure 1: Example of interaction data with block structure collected on TalkLife (left) and the corresponding network (right).

Definition 2.1 (Interaction data). For a set \mathcal{P} , let $fin(\mathcal{P})$ be the set of all finite multisets of \mathcal{P} . The interaction process of \mathcal{P} is the correspondence $\mathcal{I} : \mathbb{N} \rightarrow fin(\mathcal{P})$ between the natural numbers and finite multisets of \mathcal{P} .

Additional structure can be incorporated into Definition 2.1. In Talklife, for example, there is a single poster and multiple commentators. Definition 2.1 can capture this by replacing $fin(\mathcal{P})$ with $fin_1(\mathcal{P}) \times fin(\mathcal{P})$ where $fin_1(\mathcal{P})$ are sets of size one from \mathcal{P} . This generalization can also be extended into other types of interactions. See [7] for additional examples of these extensions.

Using Figure 1 as an example, each interaction is represented by the user who posts and the users who comment. The users, regardless of being posters or commentators, are drawn from the population $\mathcal{P} \subseteq \mathbb{N}$. The interaction process is a correspondence $\mathcal{I} : \mathbb{N} \rightarrow \text{fin}_1(\mathcal{P}) \times \text{fin}(\mathcal{P})$, i.e., $\mathcal{I}(1) = (\{a\}, \{b, c, d\})$, $\mathcal{I}(2) = (\{e\}, \{d, f\})$, and $\mathcal{I}(3) = (\{g\}, \{f, h\})$.

Individuals who post and comment are likely to exhibit latent node-level community behavior. That is, commentators and posters form a block structure. In Figure 1, for example, Users a, b, c, and d all belong to block 1, while Users f, g and h belong to block 2. Within-block interactions are more likely to be observed than between-block interactions. Note, however, that users from distinct blocks may appear within a single interaction, i.e., User f comments on a post by User e. We formalize this idea in Definition 2.2.

Definition 2.2 (Block structured interaction data). A *K-block structure* is defined as the mapping $B : \mathcal{P} \rightarrow [K]$, i.e., for all $x \in \mathcal{P}$, $B(x) \in [K]$ is the block to which x is assigned. The interaction process induced by B is called the *block interaction process*, which is the correspondence $\mathcal{I}_B : \mathbb{N} \rightarrow \text{fin}([K])$.

In the running example shown in Figure 1, $K = 2$ and the interaction process induced by B is $\mathcal{I}_B(1) = (\{1\}, \{1, 1, 1\})$, $\mathcal{I}_B(2) = (\{1\}, \{1, 2\})$, and $\mathcal{I}_B(3) = (\{2\}, \{2, 2\})$. Note that for the pre-image B^{-1} , $B^{-1}(i) \cap B^{-1}(j) = \emptyset$ if $i \neq j$, and $\cup_{i=1}^K B^{-1}(i) = \mathcal{P}$. That is, B partitions \mathcal{P} into K non-overlapping sets.

Above, interaction processes are distinct if they are defined on different populations or given distinct block structures. Here, we formally address the equivalence of networks built from two different block structured interaction processes that can be linked via a set of bijections. Let $\rho : \mathcal{P} \rightarrow \mathcal{P}'$ be the bijection which acts on I via $\rho\mathcal{I} : \mathbb{N} \rightarrow \text{fin}(\mathcal{P}')$. That is, for $(s_1, \dots, s_m) \in \text{fin}(\mathcal{P})$:

$$\rho \circ (s_1, \dots, s_m) = (\rho(s_1), \dots, \rho(s_m)) \in \text{fin}(\mathcal{P}')$$

The bijection also acts on the block structure B defining the map $\rho B := B \circ \rho^{-1} : \mathcal{P}' \rightarrow \text{fin}([K])$. Consider a second block structure, $B' : \mathcal{P}' \rightarrow \text{fin}([K])$. Then a second bijection $\rho' : [K] \rightarrow [K]$ acts on the block interaction process $I_{B'}$ via $\rho' \mathcal{I}_{B'} : \mathbb{N} \rightarrow \text{fin}([K])$. In other words, the bijection ρ' preserves the block structure but changes the block labels. With this, the interaction-labeled network with block structure B is then the equivalence class constructed from the interaction network by quotienting out over pairs of bijections (ρ, ρ') that preserve block structure:

$$\mathbf{Y}_{\mathcal{I}, B} = \bigcup_{\#\mathcal{P}' = \#\mathcal{P}} \left\{ \begin{array}{l} \mathcal{I}' : \mathbb{N} \rightarrow \text{fin}(\mathcal{P}') : \quad \rho \mathcal{I} = \mathcal{I}', \quad \text{for } \rho : \mathcal{P} \rightarrow \mathcal{P}' \\ B' : \mathcal{P}' \rightarrow [K] : \quad \rho' \mathcal{I}_{\rho B} = \mathcal{I}_{B'} \quad \text{for } \rho' : [K] \rightarrow [K] \end{array} \right\}$$

where $\#P$ is the cardinality of the population. Note we have only quotiented out labels of constituent elements and the blocks, so the network $\mathbf{Y}_{\mathcal{I}, B}$ still has uniquely labelled interactions with a unique node-level block structure. To avoid cumbersome notation, we often write \mathbf{Y} to denote the interaction-labeled network with block structure, leaving the associated interaction process I and block structure B implicit.

For any $S \subset \mathbb{N}$, we define the *restriction* of the interaction process \mathcal{I} to S by I_S . This restriction induces a restriction of the interaction labeled network \mathbf{Y} which we denote \mathbf{Y}_S . For $S = [n] = \{1, \dots, n\}$, we simply write I_n to denote the restricted structured interaction process and \mathbf{Y}_n to denote the corresponding structured interaction network. Moreover, we define the restriction of the interaction process to only the elements from a particular block b by I_b and \mathbf{Y}_b to denote the corresponding structured interaction network. In our recurring example, for instance, $I_1(2) = (\{e\}, \{d\})$ where element $\{f\}$ is removed from $I(2)$ as it belongs to block 2. This restriction is useful in defining block-specific network properties.

2.3 Exchangeable interaction-labeled networks with block structure

For any finite permutation $\sigma : \mathbb{N} \rightarrow \mathbb{N}$, let \mathcal{I}^σ denote the relabeled interaction process defined by $I^\sigma(i) = I(\sigma^{-1}(i))$ and the relabeled block interaction process defined by $I_B^\sigma(i) = I_B(\sigma^{-1}(i))$ for each $i \in \mathbb{N}$. Then y^σ denotes the corresponding interaction labeled network constructed from I^σ . Note that σ does not impact the block structure B but does impact the block structure process I_B^σ . Note that the choice of representative from the equivalence class (I, B) does not matter. The interaction relabeling by σ should not be confused with the bijections ρ and ρ' , which relabel constituent elements and block labels respectively.

In the remainder of the paper, we write \mathbf{Y} to denote the random interaction labeled network with block structure B . Interaction exchangeability is characterized by the property that the labeling of the interactions (not the constituent elements or blocks) is arbitrary. We now define block exchangeable interaction networks.

Definition 2.3 (Block exchangeable interaction networks). A random interaction labeled network with block-structure \mathbf{Y} is *exchangeable* if $\mathbf{Y}^\sigma =_D \mathbf{Y}$ for all permutations $\sigma : \mathbb{N} \rightarrow \mathbb{N}$, where $=_D$ denotes *equality in distribution*.

We say an interaction process I and its associated block interaction process B are exchangeable if its corresponding interaction labeled network is exchangeable.

2.4 Sequential description of the B-VCM model

Here we provide a sequential description of a particular family of block exchangeable interaction processes, termed the B-VCM, assuming the block structure B is observed; see Section 2.5 for why this name was chosen. For ease of comprehension, the process is described in the context of TalkLife posts assuming a *single commentator*. Suppose m posts $E_{[m]} := \{E_1, \dots, E_m\}$ have been observed along with the block assignments for each observed individual. That is, the post $j \in [m]$ is given by $E_j = (S_j, R_j)$ where $S_j \in \mathbb{N}$ is the sender

and $R_j \in \mathbb{N}$ is the commentator with the associated blocks $(B(S_j), B(R_j))$. The post E_{m+1} conditional on $E_{[m]}$ and the block structure B is constructed as follows. First, the sender's block assignment is drawn according to

$$P(B(S_{m+1}) = b \mid E_{[m]}; \omega_B) \propto \begin{cases} D_m(b) + \omega_B, & \text{if } b \in [K_m] \\ (K - K_m)\omega_B, & \text{if } b \notin [K_m] \end{cases} \quad (1)$$

where $D_m(b) = \sum_{j=1}^m I(B(S_j) = b)$ is the number of individuals from block b that have been observed in $E_{[m]}$, $K_m \leq K$ is the number of unique blocks observed in $E_{[m]}$, and $\omega_b > 0$ is a model parameter.

Let $D_m(i)$ be the number of times individual $i \in \mathbb{N}$ has been observed (either as a poster or commentator) in the first m interactions $E_{[m]}$. Similar to the Chinese Restaurant Process [20], given parameters $0 < \alpha_b < 1$ and $\theta_b > -\alpha_b$ for each $b \in [K]$, poster S_{m+1} can be either chosen from one of the previously observed nodes, or an unobserved node in block b with probability:

$$P(S_{m+1} = s \mid E_{[m]}, B(S_{m+1}) = b) \propto \begin{cases} D_m(s) - \alpha_b, & \text{if } s \in V_m \cap B^{-1}(b) \\ \theta_b + \alpha_b \sum_{i \in V_m \cap B^{-1}(b)} D_m(i), & \text{if } s \notin V_m, s \in B^{-1}(b) \end{cases} \quad (2)$$

where V_m is the set of the observed senders in the first m interactions. Given the sender, a similar process is used to choose the $(m+1)$ st commentator. The block assignment for R_{m+1} is chosen according to:

$$P(B(R_{m+1}) = b' \mid B(S_{m+1}) = b, E_{[m]}) \propto \begin{cases} D_m(b, b') + \zeta_B & \text{if } b' \in [K_{m,b}] \\ (K - K_{m,b'})\zeta_B, & \text{if } b' \notin [K_{m,b}] \end{cases} \quad (3)$$

where $D_m(b, b') = \sum_{j=1}^m [I(B(S_j) = b, B(R_j) = b')]$ is the number of interactions from block b to block b' that have been observed in $E_{[m]}$, where $K_{m,b} \leq K$ are the number of unique blocks

observed as a commentator from this block, and $\zeta_B > 0$ is a model parameter. Finally, the receiver R_{m+1} is selected with probability whose expression takes the same explicit form as that of Eq (2). Note that in the above sequential description, blocks and individuals within blocks are labelled in order of appearance.

Let \mathbf{y}_m denote the observed interaction-labelled network with block structure B after m interactions, $v(\mathbf{y}_b)$ denote the number of non-isolated vertices in \mathbf{y}_m belonging to block b , and $m(\mathbf{y}_b)$ is the total degree of block b . Then, based on the above sequential description, the probability of observing \mathbf{y}_m takes the explicit form:

$$\underbrace{\frac{[K-1]_{-1}^{K_m}}{[K\omega_B]_1^m} \prod_{b \in [K_m]} [\omega_B]_1^{D_m(b)}}_{(I)} \times \underbrace{\prod_{b \in [K_m]} \frac{[\alpha_b + \theta_b]_{\alpha_b}^{v(\mathbf{y}_b)-1}}{[\theta_b + 1]_1^{m(\mathbf{y}_b)-1}} \prod_{j \in v(\mathbf{y}_b)} [1 - \alpha_b]_1^{D_m(j)-1}}_{(II)} \times \underbrace{\prod_{b \in [K_m]} \frac{[K-1]_{-1}^{K_{m,b}}}{[K\zeta_B]_1^{m_b}} \prod_{b' \in [K_{m,b}]} [\zeta_B]_1^{D_m(b,b')}}_{(III)} \quad (4)$$

where for real number x and a , and non-negative integer N , the operation on x , $[x]_a^N = x(x+a)\dots(x+(N-1)a)$. Component (I) of (4) is the probability of an interaction initiating from block b . Component (II) of (4) is the joint distribution of all the nodes within the each block b . Component (III) of (4) is the propensity of connection between block b and b' . Proposition 2.4 proves the sequential description yields a block exchangeable interaction labelled network as desired.

Proposition 2.4. *The B-VCM with parameters $\Psi = (\omega_B, \{\theta_c, \alpha_c\}, \zeta_B)$ determines a block exchangeable interaction-labeled network for all Ψ in the parameter space.*

2.5 Statistical Properties

The B-VCM is an example of block exchangeable interaction-labeled networks. A question is whether B-VCMs represent all block exchangeable interaction labeled networks. Here, we show that this is not the case by providing a representation theorem. We focus on the

setting where each interaction (s, r) is either never observed or observed infinitely often, i.e., the “blip-free” setting [6]. This setting is most relevant to the statistical applications we consider. We then leverage this representation theorem to demonstrate connections between the proposed B-VCM and the degree-corrected stochastic block model.

We first define the $\text{fin}_2([K])$ -simplex, denoted \mathcal{F}_K , and the restricted $\text{fin}_2(\mathbb{N})$ -simplex, denoted $\mathcal{F}_{\bar{b}}$ where $\bar{b} \in \text{fin}([K])$:

$$\mathcal{F}_K := \{(f_s)_{s \in \text{fin}_2([K])} : f_s \geq 0 \text{ and } \sum_{s \in \text{fin}_2([K])} f_s = 1\}$$

$$\mathcal{F}_{\bar{b}} := \{(f'_s)_{s \in \text{fin}_2(\mathbb{N})} : B(s) = \bar{b}, f'_s \geq 0 \text{ and } \sum_{s \in \text{fin}_2(\mathbb{N}), B(s)=\bar{b}} f'_s = 1\}$$

Let ϕ_K be a probability measure on \mathcal{F}_K and define $f_K \sim \phi_K$ be the random variables drawn from the measure. For each $\bar{b} \sim f_K$, we draw $f_{\bar{b}} \sim \phi_{\bar{b}}$ a random variable drawn from a probability measure $\phi_{\bar{b}}$ on $\mathcal{F}_{\bar{b}}$. Each $\mathbf{f} := (f_K, \{f_{\bar{b}}\})$ determines a distribution on finite multisets of \mathbb{N} relative to the block structure B by

$$\text{pr}(E = (s, r) | \mathbf{f}; B) = f_K(b, b') \times f_{(b, b')}(s, r)$$

where $\bar{b} = (b, b')$, $B(s) = b$, and $B(r) = b'$. This determines a block interaction exchangeable network.

Theorem 2.5 (Representation Theorem). *Let \mathbf{Y} be the interaction exchangeable network relative to block structure B that is blip-free. Then there exists probability measures ϕ_K on \mathcal{F}_K and $\phi_{\bar{b}}$ on $\mathcal{F}_{\bar{b}}$ such that $\mathcal{Y} \sim \epsilon_\phi$ where $\phi = (\phi_K, \{\phi_{\bar{b}}\})$ and*

$$\epsilon_\phi(\cdot) = \int_{\mathcal{F}_K \times \{\mathcal{F}_{\bar{b}}\}} \epsilon_{(f_K, \{f_{\bar{b}}\})}(\cdot) \phi(df)$$

Remark 2.6. *If $K = 1$, then $f_1(1, 1) = 1$, and so we only draw $\phi_{(1,1)}$ on $\mathcal{F}_{(1,1)}$. This recovers the representation theorem for edge exchangeable networks without block structure [6].*

Theorem 2.5 presents a general framework for generating interaction exchangeable networks relative to block structure B . Proof can be found in Section A.4 of the supplementary materials. Using the representation theorem, the B-VCM corresponds to particular choices of distributions ϕ_F and $\phi_{\bar{b}}$. Specifically, the B-VCM corresponds to the following choices: (1) the propensity of block b initiating an interaction corresponds to $\pi = (\pi_1, \dots, \pi_K)$ chosen from the symmetric Dirichlet distribution with parameter $(\omega_B, \dots, \omega_B)$ on the $(K-1)$ -simplex; (2) the propensity of block b' commenting on an interaction initiated by block b corresponds to $\mathcal{B}(b, \cdot) = (\mathcal{B}(b, 1), \dots, \mathcal{B}(b, K))$ each chosen from the symmetric Dirichlet distribution with parameter (ζ, \dots, ζ_B) on the $(K-1)$ -simplex; and (3) propensities per block b the propensities per block $f_b = (f_s^{(b)})_{s \geq 1: B(s)=b}$ are chosen from the Griffiths–Engen–McCloskey (GEM) distribution with parameter (α_b, θ_b) for each $b \in [K]$. Then:

$$P(E = (s, r) \mid \pi_b, f, \mathcal{B}) = \underbrace{[\pi_b \times \mathcal{B}(b, b')]}_{(f_K)} \times \underbrace{[f_s^{(b)} \times f_r^{(b')}]_{(f_{\bar{b}})}} \quad (5)$$

Remark 2.7 (Connection to Degree-corrected SBMs). From (5), we can relate the proposed B-VCM to the degree-corrected stochastic block model (DC-SBM). The DC-SBM models adjacency matrices $A = [A_{i,j}]$ of a random graph $G = (V, E)$. The probability of an edge between node i and j according to the DC-SBM is $\mathbb{E}(A_{i,j}) = \theta_i \theta_j P(B(i), B(j))$. In (5), node-level parameters θ_i are replaced by block-specific vertex propensities $f_s^{(b)}$ and the likelihood of link between clusters $P(b, b')$ is replaced by the likelihood of initiating and then interacting with that other cluster $\pi_b \mathcal{B}(b, b')$. Note $\sum_{b'=1}^K P(b, b')$ need not sum to one but $\sum_{b'=1}^K \mathcal{B}(b, b') = 1$.

2.6 Statistical properties of B-VCM

We next highlight two key statistical properties, the first being network properties of the B-VCM and the second being an inferential consistency property under an approximate local updating rule.

2.6.1 Network Properties

For an interaction-labeled network \mathbf{Y} , let $v(\mathbf{Y})$ denote the number of non-isolated receivers; $e(\mathbf{Y})$ be the number of interactions; $M_k(\mathbf{Y})$ is the number of interactions with k receivers; $N_k(\mathbf{Y})$ is the number of receivers that appear exactly k times; and $d(\mathbf{Y}) = (d_k(\mathbf{Y}))_{k \geq 1}$ is the degree distribution where $d_k(\mathbf{Y}) = N_k(\mathbf{Y})/v(\mathbf{Y})$. These are global statistics that do not depend on the interaction labels. We define block-specific versions by superscripting each statistic by $b \in [K]$ to denote the statistic on the network \mathbf{Y}_b , i.e., each interaction restricted to those elements that belong to block b . For instance, $v^{(b)}(\mathbf{Y})$ is the number of non-isolated receivers from block b . The statistics $e^{(b)}(\mathbf{Y})$, $M_k^{(b)}(\mathbf{Y})$, $N_k^{(b)}(\mathbf{Y})$, $d^{(b)}(\mathbf{Y})$, and $d_k^{(b)}(\mathbf{Y})$ are defined similarly.

Definition 2.8 (Global and block-level sparsity). *Let $(\mathbf{Y}_m)_{m \geq 1}$ be a sequence of interaction-labeled networks for which $e(\mathbf{Y}_m) \rightarrow \infty$ as $m \rightarrow \infty$. The sequence $(\mathbf{Y}_m)_{m \geq 1}$ is sparse if*

$$\limsup_{m \rightarrow \infty} \frac{e(\mathbf{Y}_m)}{v(\mathbf{Y}_m)^{m_{\bullet}(\mathbf{Y}_m)}} = 0,$$

where $m_{\bullet}(\mathbf{Y}_m) = e(\mathbf{Y}_m)^{-1} \sum_{k \geq 1} k M_k(\mathbf{Y}_m)$ is the average arity (i.e., number of elements) of the interactions in the restricted network \mathbf{Y}_b . A non-sparse network is dense. We say the sequence $(\mathbf{Y}_m)_{m \geq 0}$ is b -locally sparse if

$$\limsup_{m \rightarrow \infty} \frac{e^{(b)}(\mathbf{Y}_m)}{v^{(b)}(\mathbf{Y}_m)^{m_{\bullet}^{(b)}(\mathbf{Y}_m)}} = 0,$$

where $m_{\bullet}^{(b)}(\mathbf{Y}_m) = e^{(b)}(\mathbf{Y}_m)^{-1} \sum_{k \geq 1} k M_k^{(b)}(\mathbf{Y}_m)$ is the average arity (i.e., number of elements from block b) of the interactions in \mathbf{Y}_m . A network that is not b -locally sparse is b -locally dense.

For $(X_n)_{n \geq 1}$ a sequence of positive random variables and $(y_n)_{n \geq 1}$ a sequence of positive non-random variables, let $X_n \simeq y_n$ indicate $\lim_{n \rightarrow \infty} X_n/y_n$ exists almost surely and equals a finite positive random variable. Theorem 2.9 shows the canonical B-VCM model may be

either globally and locally sparse and/or dense.

Theorem 2.9. *Let $(\mathbf{Y}_m)_{m \geq 1}$ be a sequence of random exchangeable interaction-labeled networks drawn from the B-VCM. Then, for all $b \in [K]$, the expected number of non-isolated vertices in \mathbf{Y}_m belonging to block b satisfies*

$$E[v^{(b)}(\mathbf{Y}_m)] \simeq \frac{\Gamma(\theta_b + 1)}{\alpha_b \Gamma(\theta_b + \alpha_b)} (\mu_b \cdot m)^{\alpha_b}$$

where μ_b is the mean arity when restricted to elements only from block $b \in [K]$. Then $1/\mu_b < \alpha_b < 1$ implies b -local sparsity for $b \in [K]$. Furthermore, $E[v(\mathbf{Y}_m)] = \sum_{b=1}^K E[v^{(b)}(\mathbf{Y}_m)] \simeq m^{\alpha_\star}$ where $\alpha_\star = \max_b \alpha_b$. Therefore, $1/\mu < \alpha_\star < 1$ implies global sparsity.

The proof can be found in Section A.2 of the supplementary materials. Theorem 2.9 establishes that the B-VCM can capture degrees of sparsity. Note that $\mu_b \leq \mu$ implies a dense network must be b -locally dense for all blocks (i.e. $\alpha_b \leq \alpha_\star \leq 1/\mu \leq 1/\mu_b$). We next turn to considerations of power-law degree distribution.

Definition 2.10 (Global power-law degree distributions). *A sequence $(\mathbf{Y}_m)_{m \geq 1}$ exhibits power-law degree distribution if for some $\gamma > 1$ the degree distributions $(d(\mathbf{Y}_m))_{m \geq 1}$ satisfy $d_k(\mathbf{Y}_m) \sim l(k)k^\gamma$ as $m \rightarrow \infty$ for all large k for some slowly varying function $l(x)$; that is, $\lim_{x \rightarrow \infty} l(tx)/l(x) = 1$ for all $t > 0$, where $a_m \sim b_m$ indicates that $a_m/b_m \rightarrow 1$ as $m \rightarrow \infty$. More precisely, $(\mathbf{Y}_m)_{m \geq 1}$ has power law degree distribution with index γ if:*

$$\lim_{k \rightarrow \infty} \lim_{m \rightarrow \infty} \frac{d_k(\mathbf{Y}_m)}{l(k)k^{-\gamma}} = 1. \quad (6)$$

We say the sequence has b -local power-law degree distribution with index γ_b if (6) holds with $d_k^{(b)}(\mathbf{Y}_m)$ replacing the global degree distribution statistic.

Theorem 2.11 establishes the power-law degree distribution for the block-specific restricted networks built from the B-VCM as well as the global network.

Theorem 2.11. *Let $(\mathbf{Y}_m)_{m \geq 0}$ obey the B-VCM sequential description in Section 2.4. For each $m \geq 1$, let $p_m(k) = N_k(\mathbf{Y}_m)/v(\mathbf{Y}_m)$ and $p_m^{(b)}(k) = N_k^{(b)}(\mathbf{Y}_m)/v^{(b)}(\mathbf{Y}_m)$ for $k \geq 1$ be the empirical global and local degree distributions. Then, for every $k \geq 1$,*

$$p_m^{(b)}(k) \sim \alpha_b k^{-(\alpha_b+1)} / \Gamma(1 - \alpha_b)$$

where $\Gamma(t) = \int_0^\infty x^{t-1} e^{-x} dx$ is the gamma function. That is, $(\mathbf{Y}_m)_{m \geq 1}$ has b -local power law degree distributions with exponents $\gamma_b = 1 + \alpha_b \in (1, 2)$ for all $b \in [K]$. Moreover, $\lim_{k \rightarrow \infty} \lim_{m \rightarrow \infty} p_m(k)/p_m^{(b_\star)}(k) = 1$ where $b_\star = \arg \max_b \alpha_b$ implying the sequence has global power law degree distribution with exponent $\gamma = 1 + \alpha_\star$.

2.6.2 Consistent recovery of block structure

In prior sections, the block structure was assumed known and observed as part of the sequential data generating process. In most real-world settings, the block structure is latent and must be recovered from the observed data. An important theoretical question is whether the estimated block structure is consistent (up to label permutation) with the true block structure. Theoretical guarantees for DC-SBMs have been well established [32, 11, 10].

Here, based on the connection to the DC-SBM as discussed in Remark 2.7, we consider an analogue of a DC-SBM setting [2] where the misspecification rate was shown to be bounded as the number of observed vertices in the adjacency graph increases. In the edge exchangeability framework, however, the asymptotics are with respect to the number of observed interactions leading to different asymptotic behavior. Specifically, Theorem 2.11 implies that even as the number of interactions grows, a significant fraction of vertices will have low degree. Therefore, we also bound the misclassification rate as a function of minimal degree. The proof can be found in Section A.1 of the supplementary materials.

Theorem 2.12. *Let $(Y_m)_{m \geq 0}$ obey the sequential description in Section 2.4 assuming $K = 2$, $\alpha_1 = \alpha_2$, and $\theta_1 = \theta_2$. Let B denote the true block assignments and $e_m : [v(\mathbf{Y}_m)] \mapsto [K]$*

denote a current labeling of the non-isolated vertices after observing m interactions. Under a symmetry condition provided in Section A.1, an approximate updating rule can be derived such that $\hat{B}(i) = 1$ if $\text{Deg}(i, 1) > \text{Deg}(i, 2)$ and $\hat{B}(i) = 2$ otherwise, where $\text{Deg}(i, b)$ is the number of interactions involving node i and an element from block b (as determined by the current labeling e_m). Let

$$M_{v(\mathbf{Y}_m)} = \inf_{\rho': [K] \rightarrow [K]} \frac{1}{v(\mathbf{Y}_m)} \sum_{i=1}^{v(\mathbf{Y}_m)} \mathbf{1}(\hat{B}(i) \neq \rho' B(i))$$

denote the misclassification rate (under potential label switching). As $m \rightarrow \infty$, for any $u \geq \frac{1}{e}$, under certain conditions on the current labeling provided in Section A.1 and the approximate updating rule we have

$$\mathbb{P}[M_{v(\mathbf{Y}_m)} \geq euP_{out}] \leq \exp[-ev(\mathbf{y}_m)P_{out}u \log u]$$

where e is Euler's number, $u > 1/e$ is a constant, and $P_{out} \rightarrow \sum_{d=1}^{\infty} \alpha B(d, \alpha+1) \exp(-d\mu_{\min}^2/4)$ as $m \rightarrow \infty$ where μ_{\min} is a constant depending on the current labeling. Specifically, restricting the misclassification rate to nodes of at least degree D_m denoted $M_{v(\mathbf{Y}_m)}^{D_m}$, it is possible to construct a sequence D_m , such that $|\{i \in v(\mathbf{Y}_m) : \text{Deg}(i) \geq D_m\}|/|v(\mathbf{Y}_m)|$ is non-empty with probability one and

$$\lim_{m(Y_m) \rightarrow \infty} \mathbb{P}[M_{v(\mathbf{Y}_m)}^{D_m} \geq \epsilon] = 0, \quad \text{for all } \epsilon > 0.$$

3 Inference

Theorem 2.12 shows that a simple updating rule can lead to consistent estimation of the latent block structure for high degree nodes. Figure 2 in Section A.5 of the supplementary materials shows empirical misclassification rate decreases rapidly as degree increases in a simulation study. The theory and empirical evidence thus suggests a potential large

misclassification rate for low degree nodes. This uncertainty motivates the consideration of a Bayesian framework to assess posterior uncertainty. Specifically, we introduce a Gibbs sampling algorithm for sampling from the posterior distribution of (Ψ, B) given observed interaction-labeled network \mathbf{Y}_m with latent block structure. We start with the discussion of the selection of priors, followed by a brief overview of the Gibbs sampling algorithm.

3.1 Selection of Priors

Here we outline an approach to choosing priors for the B-VCM parameters that admit conjugate Gibbs updates. First, consider the estimated block assignment \hat{B} . An equivalent mixture representation of the sequential description leads to the natural prior:

$$\hat{B}(i) \mid \pi \sim \text{Multinomial}(\pi_1, \dots, \pi_K); \quad \pi := (\pi_1, \dots, \pi_K) \sim \text{Dirichlet}(\omega)$$

where $\omega > 0$ is a constant, i.e., π follows a symmetric Dirichlet distribution. Next, considering equation (5), based on a similar argument and the fact that the entries in the same row of propensity matrix \mathcal{B} should sum up to 1, we propose a row-wise Dirichlet prior for the propensity matrix:

$$(\mathcal{B}(b, 1) \dots \mathcal{B}(b, K)) \sim \text{Dirichlet}(\zeta), \quad b \in [K].$$

This choice of prior does not enforce symmetry, i.e. $\mathcal{B}(b, b')$ may not equal $\mathcal{B}(b', b)$. A discussion of a prior under a symmetry constraint can be found in Section A.9 of the supplementary materials.

For the block-specific parameters $\{\alpha_b, \theta_b\}$, conjugate priors given block assignments B exists. Specifically, a conjugate prior for the power-law parameters α_b is a Beta distribution. For datasets of reasonable size, empirically we have found that the choice of hyper-parameters does not significantly affect the resulting posterior distributions. In the subsequent examples, the size of the datasets was more than sufficient to not be strongly affected by the choice of global priors. For the power-law parameter, this suggests using $\alpha_b \sim \text{Beta}(1, 1)$, i.e., the

Uniform distribution, for each $b \in [K]$. For the other parameter θ_b , we find Gamma(1,1) is an appropriate prior in both the simulations and the real world data after applying our method to the Talklife data. An alternative approach is to fit the Hollywood model [6] to the entire dataset, and get the estimate $\hat{\theta}$. In TalkLife, we found that $\hat{\theta}$ was between 1 and 2. Therefore, Gamma($\hat{\theta}$, 1) is also a reasonable choice of prior such that the mean is centered at the global fit.

3.2 Gibbs Sampling Algorithm

Here we introduce a Gibbs sampling algorithm for sampling from the posterior distribution of (Ψ, B) given an observed interaction-labeled network \mathbf{Y}_m with latent block structure B . The algorithm uses auxiliary variable methods [8] to perform conjugate updates for all parameters Ψ . Pseudo-code is provided in Algorithm 1.

Algorithm 1 Pseudo-code of Gibbs-sampling based algorithm

```

Specify  $\omega, \zeta, \delta, \mu, K$ 
Initiate  $\mathcal{B}, \{\alpha_b\}, \{\theta_b\}, \{B(i)\}$ 
for iterations do
  for  $i \in v(\mathcal{Y}_m)$  do
    Update  $B(i)$  according to Eq (7)
  end for
  for  $b \in [K]$  do
    Update  $\alpha_b$  using auxiliary variables according to Eq (9)
    Update  $\theta_b$  using auxiliary variable according to Eq (8)
  end for
  for  $b \in [K]$  do
    Update  $\mathcal{B}(b, 1) \dots B(b, K)$  according to Eq (10)
  end for
end for

```

In Algorithm 1, we first sequentially update block assignments, $\{B(i)\}_{i \in v(\mathbf{Y}_m)}$. Let $\mathcal{H}_m^{(b)} = v(\mathbf{Y}_m) \cap B^{-1}(b)$ denote all observed vertices in block $b \in [K]$. Then the probability of assigning $i \in v(\mathbf{Y}_m)$ to block $b \in [K]$ given Ψ and all other block assignments $\{B(i')\}_{i' \neq i}$ is

proportional to:

$$p_b := \underbrace{\mathcal{B}(\omega + L)}_{(I)} \times \underbrace{\frac{D_m(i)!}{\prod_b D_m(i, b)!} \prod_{b'=1}^K \mathcal{B}(b, b')^{D_m(i, b')}}_{(II)} \times \underbrace{P(\{\mathcal{H}_m^{(b)}\} | \alpha_b, \theta_b, \delta, \mu)}_{(III)} \quad (7)$$

where $L = \{L_1, \dots, L_K\}$ is the counts of the interactions initiated from block 1 to K respectively, $\mathcal{B}(\cdot)$ is the Beta function, $D_m(i)$ is the degree of node i , and $D_m(s, b)$ is the number of interactions node i has with block b . Term (I) is derived by integrating over the latent parameter π in the distribution $P(\{B(i)\} | \pi, \omega)$. Term (II) is derived by considering nodes that have connections with the node i that is being updated in the current iteration. Term (III) takes the explicit form as shown in Part II of Eq (4).

The conditional updates of α_b and θ_b is shown as follows. Given the block assignment $\{B(i)\}$, the values of α_b and θ_b can be sampled from the posterior distribution. Here, auxiliary variable methods [26] are used in a similar way as in prior inferential approaches for edge exchangeable model [7]. Then, from Eq (4), we have

$$\begin{aligned} x_b &\sim \text{Beta}(\theta_b + 1, m(\mathbf{Y}_b) - 1), b \in [K] \\ y_{i,b} &\sim \text{Bernoulli}\left(\frac{\theta_b}{\theta_b + \alpha_b \cdot i}\right), i = 1, \dots, v(\mathbf{Y}_b) - 1, b \in [K] \\ z_{s,j,b} &\sim \text{Bernoulli}\left(\frac{j-1}{j-\alpha_b}\right), s \in v(\mathbf{Y}_b), j = 1, \dots, D_m(s, b) - 1 \\ \theta_b &\sim \text{Gamma}\left(\sum_{i=1}^{v(\mathbf{Y}_b)-1} y_{i,b} + a, b - \log x_b\right) \end{aligned} \quad (8)$$

$$\alpha_b \sim \text{Beta}\left(b + \sum_{i=1}^{v(\mathbf{Y}_b)-1} (1 - y_{i,b}), d + \sum_{s \in v(\mathbf{Y}_b)} \sum_{j=1}^{D_m(b,s)-1} (1 - z_{s,j,b})\right) \quad (9)$$

where $\{a, b, c, d\}$ are the hyperparameters for the Gamma and Beta priors respectively. The difference between this algorithm and [7] is that the prior work considered hierarchical structure while here we consider latent non-overlapping communities. Last, given the block assignment $\{B(i)\}$, the row-wise update of the propensity matrix follows from the conjugate

Dirichlet prior:

$$(\mathcal{B}(b, 1) \dots \mathcal{B}(b, K)) \sim \text{Dirichlet}(D_m(b, 1) + \zeta_{b,1} \dots D_m(b, K) + \zeta_{b,K}) \quad (10)$$

for each $b \in [K]$. Convergence of Algorithm 1 can be checked via traceplots and, in our experiments, occurs within the first hundred or so iterations; see Figure 8 and Figure 9 in the supplementary materials for trace plots from our simulation and case study.

Remark 3.1 (Scalability). *Algorithm 1 may not scale well to large networks. Given $K \ll |v(\mathbf{Y})|$, the critical issue in scaling up our proposal is finding good approximate algorithms for updating block assignments. Equation (7) suggests an approximate sampling algorithm that relies on small, local node neighborhoods. Moreover, Theorem 2.12 suggests high degree nodes may have low posterior uncertainty. Both suggest a path forward via a parallel, approximate algorithm that may perform well in practice. We do not pursue this here, but we consider this important future work.*

4 Simulations

In this section, we demonstrate via simulation that Algorithm 1 performs empirically well in recovering network properties. These include (1) recoverability of the block assignment and (2) accurate estimation of the power-law parameters. At the end of this section, we propose and empirically assess a model selection criteria to identify the number of latent communities, K .

4.1 Recovering Block Assignment Labels

In this section, we assume the number of blocks is $K = 2$. The standardized L_2 norm is used as a distance metric between true block assignment and the posterior distribution over block assignments. In the i th iteration of the Gibbs sampler, let the inferred block

assignment be $\hat{B}_m^{(i)} \in \{0, 1\}^{v(\mathcal{Y}_m)}$ and $B_m \in \{0, 1\}^{v(\mathcal{Y}_m)}$ be the true block assignment. Define the standardized L_2 norm to be:

$$\mathcal{L}_m = \frac{1}{\sqrt{v(\mathbf{Y}_m)}} \left\| B_m - \frac{1}{n} \sum_{i=1}^n \hat{B}_m^{(i)} \right\|_2$$

where n is the total number of Gibbs iterations. The norm is standardized by dividing the number of nodes in the network such that the minimum (0) and maximum (1) values represent entirely correct and incorrect node assignments respectively. Note that the block labels are arbitrary; that is, when calculating the \mathcal{L}_m , one must be concerned with *label switching* [15]. Given a complete random guess, the \mathcal{L}_m norm will be approximately 0.5 as m increases. To account for potential label switching, the \mathcal{L}_m norm was calculated for the inferred block assignment $\hat{B}_m^{(i)}$ as well as its conjugate $1 - \hat{B}_m^{(i)}$ and the minimum of the two norms was taken. This leads to a range of 0 to 0.5 for the estimated distance, such that the closer the distance is to 0, the better the recovery of the community structure.

In our simulations, we consider simulated datasets with different propensity matrices and power-law parameters. We assume the power-law parameters are the same across different blocks, i.e. $\alpha_1 = \alpha_2$, and we fix $\theta_1 = \theta_2 = 5$. The number of interactions in each simulated network vary from 1000, 2500, to 10000. The probability of an interaction initiated from either block is the same, i.e. $\pi_1 = \pi_2 = 0.5$. We repeated the simulation in each setting 20 times. The mean values of the L_2 norm in different settings are shown in Table 1. Two conclusions based on the results are: (1) given the same value of the power-law parameter α and the size of the network, the lower the inter-community connection rate, the better the recovery of the block assignments; (2) as the number of observations increase, the block assignments become more accurate in almost all settings.

To empirically demonstrate the conclusion from Theorem 2.12 on high-degree nodes, we calculated the L_2 norm as a function of the degree cutoff, as shown in Figure 2. The visualization is based on the setting where $\alpha_1 = \alpha_2 = 0.5$, and the within block interaction

	# Interactions	$\mathcal{B} = \{0.1, 0.9\}$	$\mathcal{B} = \{0.3, 0.7\}$	$\mathcal{B} = \{0.5, 0.5\}$
$\alpha = \{0.1, 0.1\}$	1,000	0.043 (0.016)	0.183 (0.033)	0.458 (0.028)
	2,500	0.067 (0.096)	0.161 (0.042)	0.457 (0.023)
	10,000	0.053 (0.072)	0.226 (0.139)	0.454 (0.018)
$\alpha = \{0.3, 0.3\}$	1,000	0.075 (0.013)	0.255 (0.067)	0.475 (0.020)
	2,500	0.067 (0.008)	0.232 (0.058)	0.465 (0.037)
	10,000	0.058 (0.007)	0.232 (0.068)	0.462 (0.024)
$\alpha = \{0.5, 0.5\}$	1,000	0.104 (0.013)	0.303 (0.028)	0.466 (0.035)
	2,500	0.101 (0.008)	0.298 (0.044)	0.476 (0.019)
	10,000	0.089 (0.006)	0.295 (0.047)	0.474 (0.025)
$\alpha = \{0.7, 0.7\}$	1,000	0.184 (0.041)	0.382 (0.039)	0.474 (0.030)
	2,500	0.156 (0.012)	0.378 (0.022)	0.490 (0.009)
	10,000	0.143 (0.008)	0.348 (0.014)	0.480 (0.023)
$\alpha = \{0.9, 0.9\}$	1,000	0.388 (0.068)	0.482 (0.023)	0.484 (0.032)
	2,500	0.335 (0.034)	0.465 (0.023)	0.488 (0.012)
	10,000	0.279 (0.028)	0.454 (0.017)	0.489 (0.011)

Table 1: Standardized L2 norm of the inferred block assignments and the underlying truth in different settings. For each set with the same values of the connectivity propensity \mathcal{B} , the power-law parameters $\{\alpha_1, \alpha_2\}$, and the number of interactions ($\{1, 000, 2, 500, 10, 000\}$), we repeated the simulation 20 times. The mean values (SD) over 20 simulations are shown here.

propensity $\mathcal{B}(1, 1) = \mathcal{B}(2, 2) = 0.9$. And the L_2 norm is calculated with nodes whose degree is greater or equal to the value indicated by the x-axis. Regardless of the size of the observed network, the higher the degree, the smaller the L_2 norm, which indicates a lower misspecification rate. Meanwhile, as the number of interactions increases, the L_2 norm decreases to 0 given the same degree cutoff. See Section A.5 of the supplementary materials for similar plots for the misspecification rate as a function of the degree cutoff, which yields similar conclusions.

Note that the L_2 norm is not applicable when there are multiple blocks ($K > 2$). To overcome this potential problem, we also use the Cross Entropy Loss as a criteria to evaluate the accuracy of the block assignment (See Table 3 in Section A.8 of the supplementary materials), which gives similar conclusions. Results from simulation settings where $\alpha_1 \neq \alpha_2$ are presented in Table 4 in Section A.7.

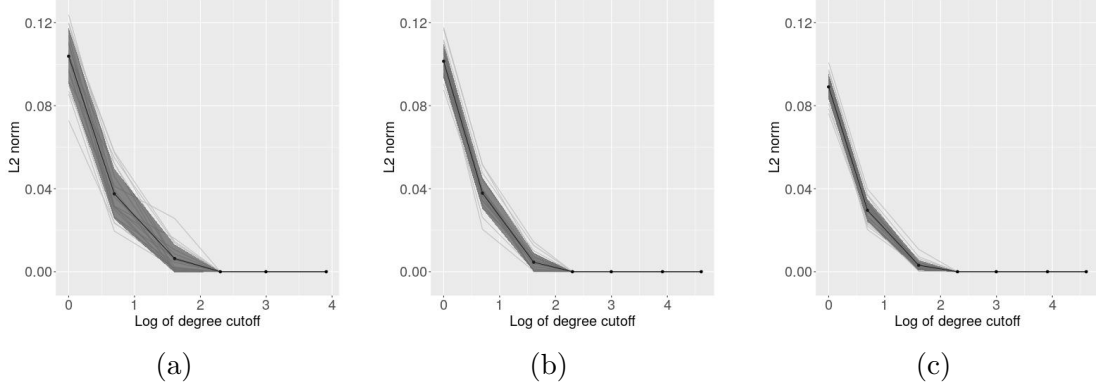


Figure 2: The L_2 norm as a function of the degree cutoff, in the setting where $\alpha_1 = \alpha_2 = 0.5$, $\mathcal{B}(1, 1) = \mathcal{B}(2, 2) = 0.9$, with (a) 1,000, (b) 2,500, and (c) 10,000 interactions presented in the network. The solid dark line is the average L_2 norm over 20 replications. The L_2 norm is calculated based on the nodes whose degree is greater or equal to the degree cutoff as indicated by the x-axis. The grey shadow indicates the SD.

4.1.1 Estimates of power-law parameters

Another important question is whether the posterior distributions adequately concentrate around the true block-specific parameters $\{\alpha_b\}_{b \in [K]}$ which controls the within-block sparsity and power-law structure. Following the same generative steps as described in Section 2.4, we simulate various networks to assess our ability to accurately estimate these parameters.

In the generative model, we set the number of blocks K equal to 2 and choose $\{\alpha_1, \alpha_2\}$ to be from the set $\{\{0.1, 0.9\}, \{0.2, 0.8\}, \{0.3, 0.7\}, \{0.4, 0.6\}\}$ and set $\theta_1 = \theta_2 = 5$. Blocks are assumed equally likely to initiate an interaction (i.e., $\{\pi_1, \pi_2\} = \{0.5, 0.5\}$). Networks of size 1,000, 10,000 and 100,000 were simulated, repeated 20 times. Given the priors specified in the previous section, the means of the posterior of the power-law parameters and the entries in propensity matrix are shown in Table 2.

First, for fixed within-block propensities and sample size, estimation accuracy is higher for larger power-law parameter values. For example, when $m = 1000$, $\{a, b\} = \{0.9, 0.1\}$ and $\{\alpha_1, \alpha_2\} = \{0.3, 0.7\}$, the power-law estimate for $\alpha_2 = 0.7$ was more accurate than the estimate for $\alpha_1 = 0.3$ (highlighted in red). This statement empirically holds even when latent communities are known. Second, power-law estimation accuracy degrades as the

inter-community connection rate increases. For example, in the 1000 interaction setting where $\{\alpha_1, \alpha_2\} = \{0.2, 0.8\}$, the power-law estimate decreases in accuracy as the likelihood of inter-community connections goes up from 0.1 to 0.5 (highlighted in yellow). Third, estimation accuracy increases as the number of interactions increase. When $\alpha_1 = 0.1$, and $\{a, b\} = \{0.9, 0.1\}$, for example, the power-law estimate becomes more accurate as the sample size grows from $N = 1,000$ to 100,000 (highlighted in blue). In Section A.10 of the supplementary materials, simulation results are presented for varying values of $\{\theta_1, \theta_2\}$.

4.1.2 The selection of K

So far we have assumed the number of communities (K) known. Here we address the selection of K . Prior solutions include but are not limited to likelihood ratio test (LRT) methods ([28], [29]), cross validation (CV) methods ([13],[12]), and Bayesian selection criteria methods ([30],[25]). Though applicable in many cases, these methods do not fit well into our current setting. LRT methods require a good distributional approximation, which is hard to find in our setting. CV methods lead to additional sampling issues and lack interpretability; and Bayesian selection criteria can be computationally expensive.

Here, we consider a model selection criteria based on the marginal posterior maximization that is similar to techniques used in the topic modeling [24]. The number of blocks is determined by choosing K that maximizes the marginal likelihood. We simulate 10,000 interactions and set the number of blocks K to be 3, 5, and 10 correspondingly. The true values of α_b are randomly chosen from Uniform(0.4, 0.8), and $\{\theta_b\}$ are all set to be 5. The intra-block connectivity is set to be $a = 0.9$, while the inter-block connectivity is set to be $b = \frac{0.1}{K-1}$. We calculate the marginal log likelihood for different K and repeat the procedure 20 times.

Figure 3 presents traceplots of the marginal log-likelihood as a function of K for each simulated dataset. In all settings, the true K gives the largest marginal likelihood, which serves as empirical evidence in support of our proposed method. Note that the likelihood

1,000 interactions	Parameters	$\{\alpha_c\} = \{0.1, 0.9\}$	$\{\alpha_c\} = \{0.2, 0.8\}$	$\{\alpha_c\} = \{0.3, 0.7\}$	$\{\alpha_c\} = \{0.4, 0.6\}$
$\{a, b\} = \{0.9, 0.1\}$	α_1	0.301 (0.182)	0.296 (0.116)	0.374 (0.08)	0.449 (0.083)
	$\tilde{\alpha}_1$	0.200 (0.100)	0.274 (0.084)	0.354 (0.068)	0.460 (0.086)
	α_2	0.886 (0.079)	0.804 (0.022)	0.712 (0.037)	0.612 (0.056)
	$\tilde{\alpha}_2$	0.904 (0.015)	0.805 (0.021)	0.714 (0.037)	0.604 (0.057)
	Diagonal	0.907 (0.020)	0.905 (0.019)	0.903 (0.019)	0.898 (0.018)
$\{a, b\} = \{0.7, 0.3\}$	α_1	0.335 (0.196)	0.335 (0.139)	0.412 (0.143)	0.501 (0.099)
	$\tilde{\alpha}_1$	0.226 (0.094)	0.256 (0.095)	0.384 (0.113)	0.470 (0.100)
	α_2	0.886 (0.069)	0.801 (0.029)	0.704 (0.061)	0.604 (0.064)
	$\tilde{\alpha}_2$	0.901 (0.015)	0.806 (0.025)	0.712 (0.061)	0.617 (0.058)
	Diagonal	0.709 (0.031)	0.710 (0.028)	0.708 (0.030)	0.708 (0.034)
$\{a, b\} = \{0.5, 0.5\}$	α_1	0.627 (0.162)	0.624 (0.185)	0.613 (0.115)	0.523 (0.124)
	$\tilde{\alpha}_1$	0.212 (0.096)	0.290 (0.079)	0.368 (0.078)	0.479 (0.105)
	α_2	0.800 (0.267)	0.726 (0.125)	0.604 (0.112)	0.555 (0.106)
	$\tilde{\alpha}_2$	0.898 (0.017)	0.804 (0.025)	0.710 (0.030)	0.601 (0.064)
	Diagonal	0.521 (0.042)	0.532 (0.051)	0.540 (0.053)	0.526 (0.050)
10,000 interactions	Parameters	$\{\alpha_c\} = \{0.1, 0.9\}$	$\{\alpha_c\} = \{0.2, 0.8\}$	$\{\alpha_c\} = \{0.3, 0.7\}$	$\{\alpha_c\} = \{0.4, 0.6\}$
$\{a, b\} = \{0.9, 0.1\}$	α_1	0.201 (0.089)	0.273 (0.083)	0.336 (0.051)	0.426 (0.042)
	$\tilde{\alpha}_1$	0.175 (0.063)	0.244 (0.063)	0.336 (0.043)	0.420 (0.039)
	α_2	0.899 (0.006)	0.799 (0.011)	0.700 (0.017)	0.605 (0.020)
	$\tilde{\alpha}_2$	0.900 (0.006)	0.800 (0.011)	0.701 (0.017)	0.607 (0.019)
	Diagonal	0.900 (0.006)	0.900 (0.006)	0.901 (0.006)	0.900 (0.006)
100,000 interactions	Parameters	$\{\alpha_c\} = \{0.1, 0.9\}$	$\{\alpha_c\} = \{0.2, 0.8\}$	$\{\alpha_c\} = \{0.3, 0.7\}$	$\{\alpha_c\} = \{0.4, 0.6\}$
$\{a, b\} = \{0.9, 0.1\}$	α_1	0.157 (0.063)	0.242 (0.054)	0.322 (0.034)	0.413 (0.025)
	$\tilde{\alpha}_1$	0.136 (0.045)	0.220 (0.040)	0.319 (0.027)	0.412 (0.022)
	α_2	0.900 (0.002)	0.799 (0.004)	0.700 (0.006)	0.604 (0.012)
	$\tilde{\alpha}_2$	0.900 (0.002)	0.799 (0.004)	0.700 (0.006)	0.605 (0.011)
	Diagonal	0.900 (0.002)	0.900 (0.002)	0.900 (0.002)	0.900 (0.002)

Table 2: Posterior means (SD) of power-law parameters $\{\alpha_c\}$ and within/between block propensity $\{a, b\}$ in different settings. To assess uncertainty due to latent communities, we also infer the posteriors of power-law parameters given true block assignments, denoted $\tilde{\alpha}_c$, $c \in [K]$. Three main conclusions are highlighted in red, yellow, and blue correspondingly.

is also affected by the underlying power-law properties of the network and the strength of the inter/intra connectivity (a and b) of different blocks as shown in Figure 3 in the supplementary materials.

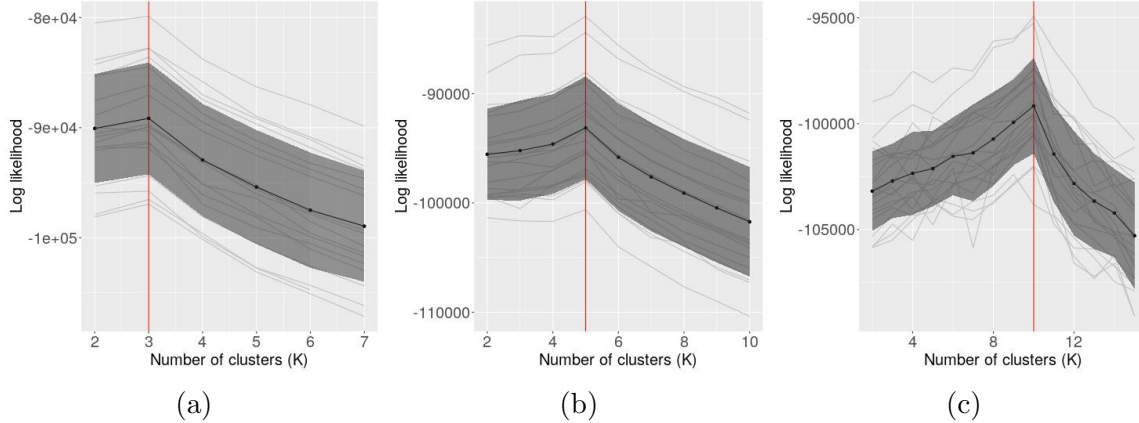


Figure 3: The trace plot of the log likelihood when the underlying true number of blocks is (a) $K=3$, (b) $K=5$, and (c) $K=10$. The grey lines represent results from 20 simulated datasets. The black line is their average. The red vertical line indicates the underlying true number of blocks in the generative model.

5 Case Study

5.1 Data overview

In this section, we apply the B-VCM to the TalkLife dataset which consists of millions of user posts and comments. Here we consider all non-deleted posts on TalkLife during the year 2019. TalkLife deploys a series of classification algorithms to determine whether a post can be flagged as including language related to one of several mental health topics. For example, a post could be flagged as *Anxiety Panic Fear Suspected* if the corresponding classifier was triggered by the text of the post. Posts that are not tagged by any one of the 33 classifiers are removed, leading to a final dataset consisting 1,481,296 posts with an average of 2.83 comments, summing up to 4,194,609 post-comment pairs. Figures 10 and 11 in the supplementary materials highlight overlap among classifiers, which shows that most posts are only flagged by a single classifier and very few users have posts that are flagged by multiple classifiers.

Figure 4 shows the global degree distribution for posts, and the distribution for subsets of posts flagged by 4 out of 33 different classifiers. The power-law degree distribution is apparent in the overall network of 2019, as well as the classifier-specific sub-networks.

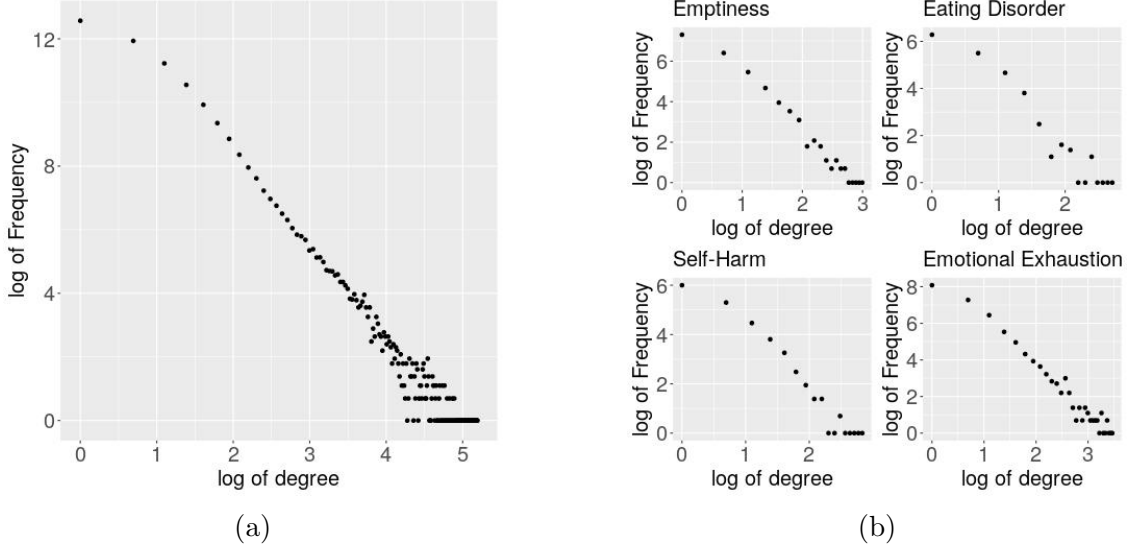


Figure 4: (a) Overview of the degree distribution of 2019 senders; (b) Degree distribution of the 2019 senders in sub-networks.

5.2 Inferring Block-labels

In this section, we aim to identify the community structure of TalkLife’s users. While the sequential description in Section 2.4 assumed a single commentator, TalkLife posts consists of multiple commentators per post. To address this, we naturally extend the B-VCM model by generating additional commentators according to the exact same procedure. Using (5), this is equivalent to a conditional independence assumption given asymptotic propensities:

$$P(E = (s, \{r_1, \dots, r_k\}) \mid \pi_c, f, \mathcal{B}) = \pi_b \times f_s^{(b)} \times \prod_{l=1}^k \mathcal{B}(b, b_l') \times \times f_{r_l}^{(b_l')}. \quad (11)$$

Based on preliminary data analysis, the machine learning generated tags partition users into non-overlapping sub-communities. Therefore, we subset the data based on these machine learning generated tags and run the Gibbs-sampling algorithm to learn the latent community structure within each sub-community. We apply the maximal marginal likelihood method in Section 4.1.2 to infer the block assignments of each user over a range of the number of blocks, K .

We next investigate the within and the between block connectivity of the inferred com-

munities. Let the block assignment of each node be a binary variable indicating the maximal hits of the blocks in the Gibbs iterations. Using Alcohol and Substance Abuse network as an example, the connectivity of the detected communities when K is set to be 2, 6, and 10 is shown in Figure 5a, 5b, and 5c. It is consistently observed that within-community connectivity is greater than the between-community connectivity. Note that B-VCM infers one larger community across different K values. To check if this is the same community across K values, we compared the overlapping of unique nodes when $K=2$, 6, and 10. The proportion is defined as $\frac{\text{Number of nodes present in both groups}}{\text{Number of nodes present in either of the groups}}$. The proportion of the overlapping nodes are 0.58, 0.58, and 0.98 when comparing $K=2$ to $K=6$; $K=2$ to $K=10$; and $K=6$ to $K=10$ correspondingly. This provides empirical evidence that the algorithm is finding sub-communities from this larger block as K increases.

5.3 Comparison with Other Methods

Here we compare our method with the spectral clustering method [27, 18] and DC-SBM [16, 9]. To apply spectral clustering, the interaction data is converted into a binary graph where an edge exists if there was an interaction between the two individuals. The connectivity of the communities detected by the spectral clustering method in Alcohol and Substance Abuse network is shown in Figure 5d, 5e, and 5f. The spectral clustering method consistently learns two large blocks. The proportion of the overlapping nodes in the largest community detected by spectral clustering are 0.99, 0.99, and 0.99 when comparing $K=2$ to $K=6$; $K=2$ to $K=10$; and $K=6$ to $K=10$ respectively. This indicates little variation in the inferred community structure across values of K . We compare the overlapping of nodes clustered in the largest block by B-VCM and the largest two blocks by spectral clustering. The overlapping proportion of the nodes are 0.62, 0.91, 0.90 when $K=2$, 6, and 10 respectively.

We then fit the degree corrected stochastic block model (DC-SBM) to the same binary graph. The connectivity of the communities detected by the DC-SBM in Alcohol and Substance Abuse network is shown in Figure 5g, 5h, and 5i in the supplementary materials.

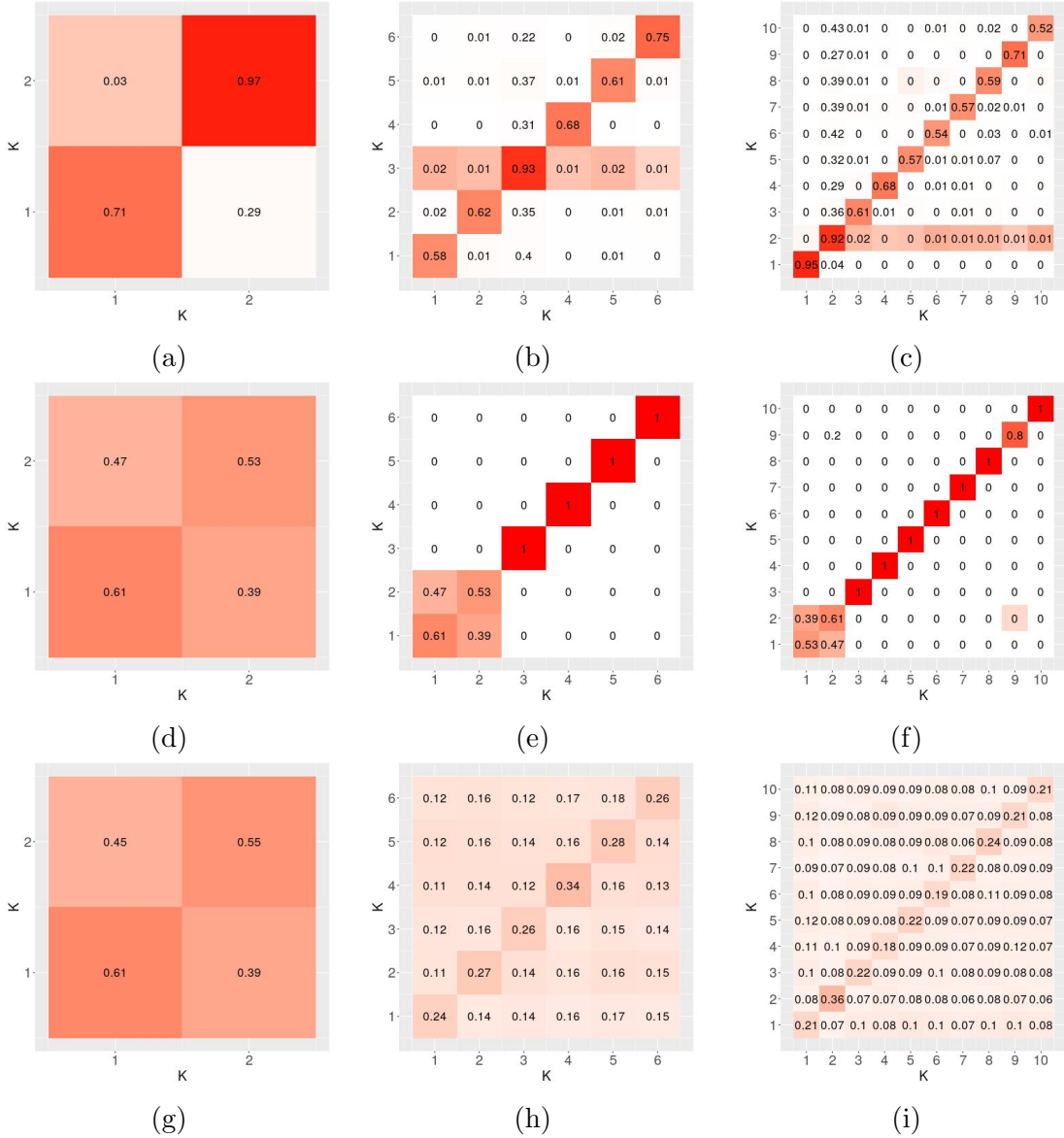


Figure 5: The inter/intra connectivity of the communities detected by B-VCM ((a)(b)(c)), the spectral clustering ((d)(e)(f)), and the degree corrected stochastic block model ((g)(h)(i)), ranging from 0 to 1, indicates the proportion of the interactions that initiated from one block to the other. The number within each cell is the proportion of the interactions initiated from one cluster (y-axis) to another (x-axis), normalized by each row.

While the sizes of the DC-SBM inferred communities are much more balanced, the within-compared to between-community connectivity is much weaker. Users that were part of the largest B-VCM inferred block are distributed across different DC-SBM inferred blocks, indicating strong differences in inferred community structure. To assess sensitivity to the projection onto a binary graph based on existence of a single interaction, the DC-SBM was fit to a projected network where an edge exists if the number of interactions between the two nodes is greater than or equal to two. This projection had 13% of the edges of the original binary graph. The results are shown in Section A.14 of the supplementary materials.

To further assess the quality of the inferred latent community structure, we investigate the inferred block consistency over time. We split the data into two halves based on whether the post occurred before June 30th, and infer the latent community structure within each time window using all three approaches. The Hellinger distance is used to quantify the difference between the block assignments, which is defined as:

$$HL = \frac{1}{v(\mathbf{Y})} \sum_{i=1}^{v(\mathbf{y})} \frac{1}{\sqrt{2}} \sqrt{\sum_{k=1}^K (\sqrt{p_{ki}} - \sqrt{q_{ki}})^2}$$

where K is the number of presumed blocks, and $v(\mathbf{Y})$ is the number of nodes; p and q correspond to the probability vector of a node belonging to each of the K blocks. To overcome the label switching problem, we perform a greedy matching of blocks by size, starting with the largest communities, followed by the second largest, and so on so forth.

For illustrative purposes we use Alcohol and Substance Abuse network and Behavioral Symptoms network as two examples. The results are shown in Figure 6 (See Section A.13 of the supplementary materials for results in other example networks). For the two subnetworks, the marginal likelihood is maximized when $K = 2$ and 4 respectively. Due to uncertainty in K , we present a range of values. The Hellinger Distance of inferred blocks assignments using our proposed method is smallest at these of optimal K valued based on marginal likelihood. Moreover, when comparing to inferred block assignments using spectral clustering and DC-

SBM, the Hellinger Distance is smaller using our proposed method for all choices of K , which indicates the communities detected by our method are more consistent over time than the communities detected by the other two methods.

6 Discussion

In this paper, we have proposed a new class of exchangeable interaction models that allow for node-level community structure. The framework models networks arising from the interaction process perspective and allows for networks that exhibit power-law degree distributions and network sparsity. We provide theoretical guarantees that the network sparsity can be retained in both the block-specific sub-networks and the entire network. We also prove that the misspecification rate of the inferred block assignments can be bounded, with the bound decreasing rapidly for high degree nodes. We implement the proposed B-VCM using a Gibbs sampling approach and demonstrate the efficacy of our algorithm through simulation. We end by applying our method to the TalkLife data to identify online user communities. We compare our results with inferred communities based on spectral clustering and degree-corrected stochastic block models, demonstrating more interpretable clustering results and consistency of the clusters over time.

There are numerous directions for future work. First, our proposed framework considered node-level community detection. Interaction processes may also exhibit clustering of different types of interactions (e.g., latent interaction topics). Second, given the size of modern interaction data, as discussed in Remark 3.1 there is a need to consider scalable implementations of the proposed algorithm or alternative algorithms that can handle hundreds of millions to billions of interactions [4]. Third, our model assumes conditional independence of interactions given block assignments and node-level propensities. Recent work has considered community detection with dependent connectivity [31]. A natural question how to incorporate such dependency into the interaction exchangeable framework.

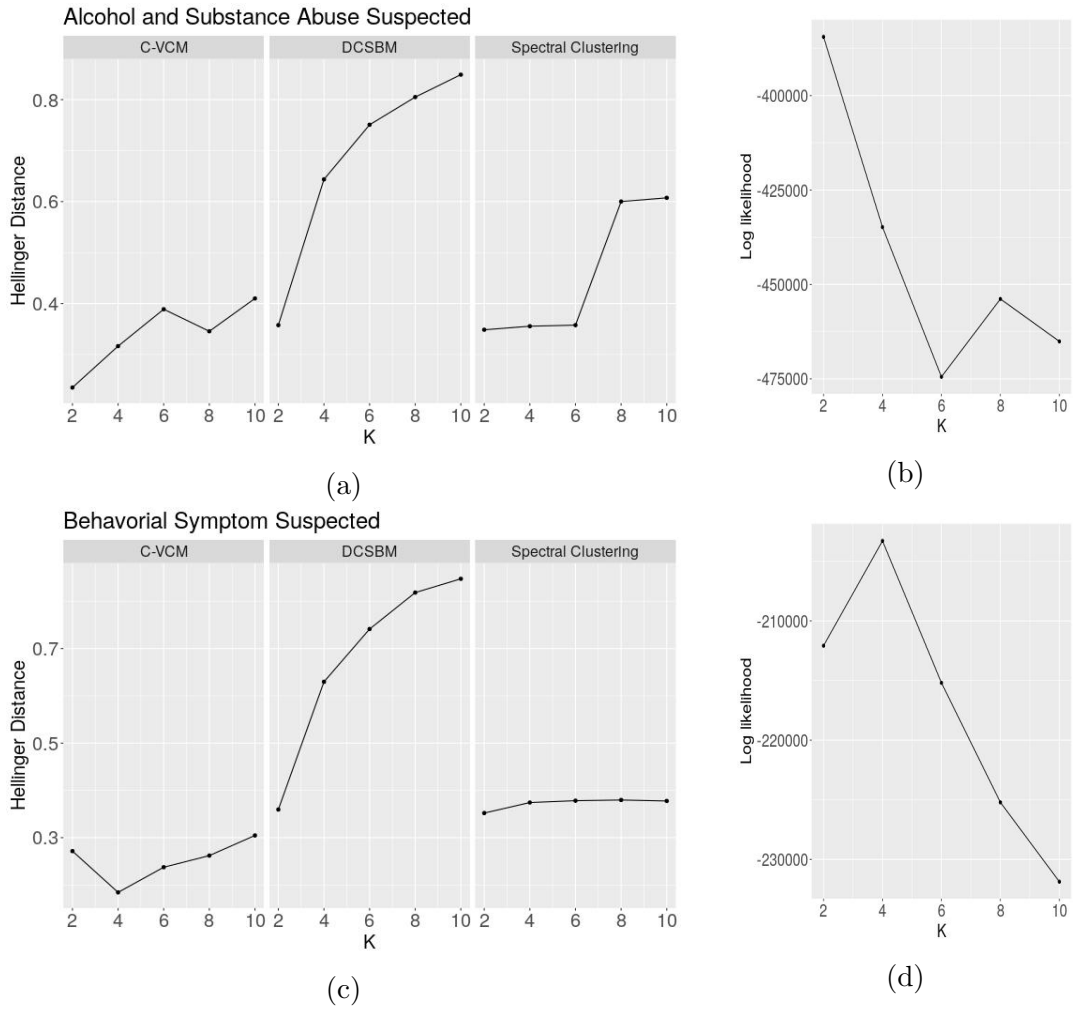


Figure 6: The Hellinger distances of the block assignment between the first half and the second half of the 2019 data in (a) Alcohol and Substance Abuse suspected network and (c) Behavioral Symptoms Suspected network. The marginal likelihood over different K values in (b) Alcohol and Substance Abuse suspected network and (d) Behavioral Symptoms Suspected network.

References

- [1] Lada A Adamic et al. “Search in power-law networks”. In: *Physical review E* 64.4 (2001), p. 046135.
- [2] Arash A Amini et al. “Pseudo-likelihood methods for community detection in large sparse networks”. In: *The Annals of Statistics* 41.4 (2013), pp. 2097–2122.
- [3] Peter Chin, Anup Rao, and Van Vu. “Stochastic block model and community detection in sparse graphs: A spectral algorithm with optimal rate of recovery”. In: *Conference on Learning Theory*. PMLR. 2015, pp. 391–423.
- [4] Julien Chiquet, Stephane Robin, and Mahendra Mariadassou. “Variational inference for sparse network reconstruction from count data”. In: *International Conference on Machine Learning*. PMLR. 2019, pp. 1162–1171.
- [5] Harry Crane and Walter Dempsey. “A Statistical Framework for Modern Network Science”. In: *Statistical Science* 36.1 (2021), pp. 51–67. DOI: [10.1214/19-STS759](https://doi.org/10.1214/19-STS759). URL: <https://doi.org/10.1214/19-STS759>.
- [6] Harry Crane and Walter Dempsey. “Edge exchangeable models for network data”. In: *arXiv preprint arXiv:1603.04571* (2016).
- [7] Walter Dempsey, Brandon Oselio, and Alfred Hero. “Hierarchical network models for exchangeable structured interaction processes”. In: *Journal of the American Statistical Association* (2021), pp. 1–18.
- [8] M. Escobar and M. West. “Bayesian density estimation and inference using mixtures”. In: *Journal of the American Statistical Association* 90 (1995), pp. 577–588.
- [9] Thorben Funke and Till Becker. “Stochastic block models: A comparison of variants and inference methods”. In: *PloS one* 14.4 (2019), e0215296.
- [10] Chao Gao, Yu Lu, and Harrison H Zhou. “Rate-optimal graphon estimation”. In: *The Annals of Statistics* 43.6 (2015), pp. 2624–2652.

- [11] Chao Gao et al. “Community detection in degree-corrected block models”. In: *The Annals of Statistics* 46.5 (2018), pp. 2153–2185.
- [12] Justin Grimmer. “A Bayesian hierarchical topic model for political texts: Measuring expressed agendas in Senate press releases”. In: *Political Analysis* 18.1 (2010), pp. 1–35.
- [13] Bettina Grün and Kurt Hornik. “topicmodels: An R package for fitting topic models”. In: *Journal of statistical software* 40.1 (2011), pp. 1–30.
- [14] Paul W Holland, Kathryn Blackmond Laskey, and Samuel Leinhardt. “Stochastic blockmodels: First steps”. In: *Social networks* 5.2 (1983), pp. 109–137.
- [15] Ajay Jasra, Chris C Holmes, and David A Stephens. “Markov chain Monte Carlo methods and the label switching problem in Bayesian mixture modeling”. In: *Statistical Science* (2005), pp. 50–67.
- [16] Brian Karrer and Mark EJ Newman. “Stochastic blockmodels and community structure in networks”. In: *Physical review E* 83.1 (2011), p. 016107.
- [17] Morten Mørup and Mikkel N Schmidt. “Bayesian community detection”. In: *Neural computation* 24.9 (2012), pp. 2434–2456.
- [18] Andrew Y Ng, Michael I Jordan, and Yair Weiss. “On spectral clustering: Analysis and an algorithm”. In: *Advances in neural information processing systems*. 2002, pp. 849–856.
- [19] SL van der Pas and AW38078661407 van der Vaart. “Bayesian community detection”. In: *Bayesian Analysis* 13.3 (2018), pp. 767–796.
- [20] Jim Pitman et al. *Combinatorial stochastic processes*. Tech. rep. Technical Report 621, Dept. Statistics, UC Berkeley, 2002. Lecture notes for . . . , 2002.
- [21] Maoying Qiao et al. “Adapting stochastic block models to power-law degree distributions”. In: *IEEE transactions on cybernetics* 49.2 (2018), pp. 626–637.

- [22] Karl Rohe, Sourav Chatterjee, and Bin Yu. “Spectral clustering and the high-dimensional stochastic blockmodel”. In: *The Annals of Statistics* 39.4 (2011), pp. 1878–1915.
- [23] David Strauss and Michael Ikeda. “Pseudolikelihood estimation for social networks”. In: *Journal of the American statistical association* 85.409 (1990), pp. 204–212.
- [24] Matt Taddy. “On estimation and selection for topic models”. In: *Artificial Intelligence and Statistics*. PMLR. 2012, pp. 1184–1193.
- [25] Yee W Teh, David Newman, and Max Welling. *A collapsed variational Bayesian inference algorithm for latent Dirichlet allocation*. Tech. rep. CALIFORNIA UNIV IRVINE SCHOOL OF INFORMATION and COMPUTER SCIENCE, 2007.
- [26] Yee Whye Teh. “A Bayesian interpretation of interpolated Kneser-Ney”. In: (2006).
- [27] Hadrien Van Lierde, Tommy WS Chow, and Guanrong Chen. “Scalable spectral clustering for overlapping community detection in large-scale networks”. In: *IEEE Transactions on Knowledge and Data Engineering* 32.4 (2019), pp. 754–767.
- [28] Quang H Vuong. “Likelihood ratio tests for model selection and non-nested hypotheses”. In: *Econometrica: Journal of the Econometric Society* (1989), pp. 307–333.
- [29] YX Rachel Wang and Peter J Bickel. “Likelihood-based model selection for stochastic block models”. In: *The Annals of Statistics* 45.2 (2017), pp. 500–528.
- [30] Xiaoran Yan. “Bayesian model selection of stochastic block models”. In: *2016 IEEE/ACM International Conference on Advances in Social Networks Analysis and Mining (ASONAM)*. IEEE. 2016, pp. 323–328.
- [31] Yubai Yuan and Annie Qu. “Community Detection with Dependent Connectivity”. In: *arXiv preprint arXiv:1812.06406* (2018).
- [32] Yunpeng Zhao, Elizaveta Levina, and Ji Zhu. “Consistency of community detection in networks under degree-corrected stochastic block models”. In: *The Annals of Statistics* 40.4 (2012), pp. 2266–2292.

Supplementary materials for “Node-level community detection within edge exchangeable models for interaction processes”

A Appendix

A.1 Proof of Theorem 2.12—Two cluster scenario

Given an initial labeling $e : v(\mathbf{Y}_m) \rightarrow [K]$ of all observed nodes in the network \mathbf{Y}_m , our goal is to show the misclassification rate (accounting for label switching) is bounded after a single iteration of an updating algorithm that approximately maximizes the likelihood given initial labeling. Specifically, we will show the misclassification rate decays rapidly and is therefore small for high-degree nodes.

Conditional on the asymptotic frequency of initiating an interaction and the propensity matrix, π and \mathcal{B} respectively, the B-VCM likelihood $P(\mathbf{Y}_m = \mathbf{y}_m | \{\alpha_b, \theta_b\}, \pi, \mathcal{B}, \{B(i)\}_{i \in v(\mathbf{Y}_m)})$ is given by:

$$\prod_{b=1}^K \pi_b^{L_b} \times \frac{[\alpha_b + \theta_b]_{\alpha_b}^{v(\mathbf{y}_b)-1}}{[\theta_b + 1]_1^{m(\mathbf{y}_b)-1}} \prod_{j \in \mathcal{H}_m^{(b)}} [1 - \alpha_b]_1^{D_m(j,b)-1} \times \prod_{b'=1}^K \mathcal{B}(b, b')^{D_m(b,b')} \quad (1)$$

where L_b is the number of interactions initiated by cluster $b \in [K]$, $v(\mathbf{y}_b)$ is the number of non-isolated vertices from cluster b , $m(\mathbf{y}_b) = \sum_{j \in v(\mathbf{y}_b)} D_m(j, b)$ is the number of times

(with multiplicity) that the cluster b nodes are observed, $D_m(j, b)$ is the degree of node j in cluster b , and $D_m(b, b')$ is the number of interactions between cluster b and b' .

Assumption A.1. In the proof below, we consider the setting where $K = 2$, $a = \mathcal{B}(1, 1) = \mathcal{B}(2, 2)$, $b = \mathcal{B}(1, 2) = \mathcal{B}(2, 1)$, $\alpha_1 = \alpha_2$, $\theta_1 = \theta_2$, $\pi_1 = \pi_2$, and $a > b$. We call this a *balanced setting* since the likelihood of initiating an interaction and power-law degree distributions are equal across clusters.

Directed network setting We start by considering a *directed* version of the B-VCM in which out- and in-degree labels are distinct. Let $Deg_{out}(i)$ be the out-degree of node i , and $Deg_{out}(i, 1)$ and $Deg_{out}(i, 2)$ be the degree of node i being connected to nodes in cluster 1 and 2 correspondingly according to labeling e . Then, based on a directed version of (1), the log likelihood of assigning the node i to cluster 1 is:

$$\begin{aligned}
l_{i,1} = & (Deg_{out}(i) + L_{1,-i}) \log \pi_1 + \log[\mathcal{B}(1, 1)^{D_m(1,1)} \mathcal{B}(1, 2)^{D_m(1,2)}] \\
& + (L_{2,-i}) \log \pi_2 + \log[\mathcal{B}(2, 1)^{D_m(2,1)} \mathcal{B}(2, 2)^{D_m(2,2)}] \\
& + \log \left[\frac{[\alpha_1 + \theta_1]_{\alpha_1}^{v_{-i}(\mathbf{y}_1)}}{[\theta_1 + 1]_1^{m_{-i}(\mathbf{y}_1) + Deg_{out}(i) - 1}} \prod_{j \in \mathcal{H}_m^{(1)}, j \neq i} [1 - \alpha_1]_1^{D_m(j,1) - 1} [1 - \alpha_1]_1^{Deg_{out}(i) - 1} \right] \\
& + \log \left[\frac{[\alpha_2 + \theta_2]_{\alpha_2}^{v_{-i}(\mathbf{y}_2) - 1}}{[\theta_2 + 1]_1^{m_{-i}(\mathbf{y}_2) - 1}} \prod_{j \in \mathcal{H}_m^{(2)}, j \neq i} [1 - \alpha_1]_1^{D_m(j,2) - 1} \right]
\end{aligned}$$

where the subscript $-i$ denotes the statistic with node i removed. That is, $L_{b,-i}$ is the number of interactions initiated by a node in cluster $b = 1, 2$ according to the labeling e , excluding node i ; $v_{-i}(\mathbf{y}_b)$ is the number of nodes in block b excluding node i ; and $m_{-i}(\mathbf{y}_b)$ is the number of interactions in block b excluding node i . Similarly, the log likelihood of

assigning node i to cluster 2 is;

$$\begin{aligned}
l_{i,2} = & L_{1,-i} \log \pi_1 + \log[\mathcal{B}(1, 1)^{D_m(1,1)} \mathcal{B}(1, 2)^{D_m(1,2)}] \\
& + [Deg_{out}(i) + (L_{2,-i})] \log \pi_2 + \log[\mathcal{B}(2, 1)^{D_m(2,1)} \mathcal{B}(2, 2)^{D_m(2,2)}] \\
& + \log \left[\frac{[\alpha_1 + \theta_1]_{\alpha_1}^{v_{-i}(\mathbf{y}_1) - 1}}{[\theta_1 + 1]_1^{m_{-i}(\mathbf{y}_1) - 1}} \prod_{j \in \mathcal{H}_m^{(1)}, j \neq i} [1 - \alpha_1]_1^{D_m(j,1) - 1} \right] \\
& + \log \left[\frac{[\alpha_2 + \theta_2]_{\alpha_2}^{v_{-i}(\mathbf{y}_2)}}{[\theta_2 + 1]_1^{m_{-i}(\mathbf{y}_2) + Deg_{out}(i) - 1}} \prod_{j \in \mathcal{H}_m^{(2)}, j \neq i} [1 - \alpha_1]_1^{D_m(j,2) - 1} [1 - \alpha_2]_1^{Deg_{out}(i) - 1} \right].
\end{aligned}$$

Under Assumption A.1, the difference in the log likelihoods simplifies:

$$\begin{aligned}
l_{i,1} - l_{i,2} = & (\log a - \log b)(Deg_{out}(i, 1) - Deg_{out}(i, 2)) \\
& + \log \frac{\alpha_1 + \theta_1 + (v_{-i}(y_1) - 1)\alpha_1}{\alpha_2 + \theta_2 + (v_{-i}(y_2) - 1)\alpha_2} - \sum_{j=1}^{Deg_{out}(i)} \log \frac{\theta_1 + 1 + m_{-i}(y_1) + j - 2}{\theta_2 + 1 + m_{-i}(y_2) + j - 2} \quad (2)
\end{aligned}$$

Under Assumption A.1, $\theta_1 = \theta_2$ and $\alpha_1 = \alpha_2$ implies $v_{-i}(\mathbf{y}_1) \simeq v_{-i}(\mathbf{y}_2)$. Moreover, the balanced design, i.e., $b := \mathcal{B}(1, 2) = \mathcal{B}(2, 1)$, $a = \mathcal{B}(1, 1) = \mathcal{B}(2, 2)$ and $\pi_1 = \pi_2$, implies $m_{-i}(\mathbf{y}_1) \simeq m_{-i}(\mathbf{y}_2)$. Based on the Eq. 2 and the above discussion, a natural approximate updating rule is $\hat{B}(i) = 1$ if $Deg_{out}(i, 1) > Deg_{out}(i, 2)$ for each node i and $\hat{B}(i) = 2$ otherwise. Next, let $\xi_j(e_{out})$ for $j \in v(\mathbf{y})$ such that $\xi_j(e_{out}) = -1$ if $e_{out,j} = 1$ and $\xi_j(e_{out}) = 1$ if $e_{out,j} = 2$. Then define $\epsilon_{out,i} := \sum_j D_m(i, j) \xi_j(e_{out})$, where $D_m(i, j)$ is the number of directed interactions (i, j) in \mathbf{y} , i.e., initiated by node i who interacts with node j . Then the updating rule leads to correct specification of the node (i.e., the assigned label $\mathcal{B}(1)$ equals the true label $\mathcal{B}(1) = 1$) if $\epsilon_{out,i} < 0$. Thus bounding the probability of misclassifying node i is equivalent to bounding $P(\epsilon_{out,i} > 0)$.

To bound this probability, we rely on the representation theorem applied to the B-VCM which guarantees conditional independence of the interactions given the node propensities. Let $W_i^{(b)}$ denote the stick-breaking propensities for observed vertices $i \in v(\mathbf{y}_b)$. Then, given the observed set of vertices, we can construct the propensity of observing a specific node i

in block b as $f_i^{(b)} := W_i^{(b)} / \sum_{i' \in v(\mathbf{y}_b)} W_{i'}^{(b)}$. Let $\{J_1\}$ be the set of nodes that match to the truth under e , and $\{J_2\}$ be the set of nodes that do not match to the truth under e . Given the out degree of each node i , $Deg_{out}(i)$ and the propensities $\{f_i^{(b)}\}$,

$$\begin{aligned} \mathbb{E}(\epsilon_{out,i}) &= -Deg_{out}(i) \left(a \sum_{j \in \{J_1\}} f_j^{(1)} + b \sum_{j \in \{J_2\}} f_j^{(2)} - b \sum_{j \in \{J_1\}} f_j^{(2)} - a \sum_{j \in \{J_2\}} f_j^{(1)} \right) \\ &= -Deg_{out}(i) \left[a \left(\sum_{j \in \{J_1\}} f_j^{(1)} - \sum_{j \in \{J_2\}} f_j^{(1)} \right) - b \left(\sum_{j \in \{J_1\}} f_j^{(2)} - \sum_{j \in \{J_2\}} f_j^{(2)} \right) \right]. \end{aligned}$$

Let $\gamma_b = \sum_{j \in J_1} f_j^{(b)} \in [0, 1]$ denote the weighted fraction of nodes that are correctly specified and note that $\sum_{j \in J_1} f_j^{(b)} + \sum_{j \in J_2} f_j^{(b)} = 1$. Let $\mu_{1,2} := a(2\gamma_1 - 1) - b(2\gamma_2 - 1)$ then

$$Var(\epsilon_{out,i}) = 4Deg_{out}(i)[\mu_{1,2}(1 - \mu_{1,2})] \leq Deg_{out}(i)$$

Bernstein's inequality states that for a sequence of *independent* random variables (X_1, \dots, X_n) with means (μ_1, \dots, μ_n) , such that $|X_i| \leq M$, for $t \geq 0$ we have:

$$P \left(\sum_{i=1}^n (X_i - \mu_i) \geq t \right) \leq \exp \left(-\frac{t^2}{2(\sum_{i=1}^n Var(X_i) + tM'/3)} \right)$$

where $M' = M + \max_i |\mu_i|$. Recall $\epsilon_{out,i} = \sum_j D_m(i, j) \xi_j(e_{out})$ which consists of independent random variables given the propensities $\{f_j^{(b)}\}$ with mean μ and variance bounded by 1. Then, by Bernstein's inequality, we have

$$P(\epsilon_{out,i} > \mathbb{E}(\epsilon_{out,i}) + t) \leq \exp \left(-\frac{t^2}{2(Deg_{out}(i) + 2t/3)} \right) \quad (3)$$

for any $t \geq 0$.

Construction of a necessary assumption on γ_b . To set the RHS of the LHS inequality in (3) equal to 0 requires $t = -\mathbb{E}(\epsilon_{out,i}) = Deg_{out}(i)\mu_{1,2}$ which requires $\mu_{1,2} > 0$ since $t \geq 0$.

When considering node i in cluster 2, this implies a positivity condition $\mu_{2,1} > 0$. Combining Assumption A.1 that $a > b$ and $a + b = 1$ with the above positivity conditions, we arrive at the following set of conditions on γ_b :

Assumption A.2 (Positivity). *Assume (a) $\gamma_b \in (1/2, 1]$ for $b = 1, 2$, i.e., the weighted fraction of nodes that are correctly specified is greater than $1/2$; and (b) that $\{\gamma_1, \gamma_2\}$ satisfy*

$$\mu_{1,2} \wedge \mu_{2,1} =: \mu_{\min} = 2 \cdot a \left(2 \frac{\gamma_{\min} + \gamma_{\max}}{2} - 1 \right) - (2\gamma_{\max} - 1) > 0 \quad (4)$$

where $\gamma_{\min} = \gamma_1 \wedge \gamma_2$ and $\gamma_{\max} = \gamma_1 \vee \gamma_2$.

Assumption A.2(a) can be guaranteed by label switching, i.e., if e has $\gamma_b < 1/2$ then switching all labels in block b will yield an e' with $\gamma'_b := 1 - \gamma_b > 1/2$. Assumption A.2(b) guarantees positivity of both $\mu_{1,2}$ and $\mu_{2,1}$ which is necessary for the labelling e to guarantee a bound via Bernstein's inequality. In [amini2013pseudo], the proof required a *balance condition*, i.e., the fraction of nodes correctly labelled by e is constant across the two clusters). The equivalent balance condition in our setting would be $\gamma_1 = \gamma_2$, i.e., the weighted fraction of nodes correctly labelled by e is constant across the two clusters. This balance condition immediately implies (4) but is a much stronger assumption. Here we rely on the weaker assumption of approximate balance which allows these fractions to be unequal but the level of imbalance depends on the connectivity parameter a .

Lemma A.3. *For each $i \in v(\mathbf{y})$, given $Deg_{out}(i)$ and propensities $\{f_i^{(b)}\}$, then under Assumption A.1 and A.2 we have*

$$P(\epsilon_{out,i} > 0) \leq \exp\left(-\frac{Deg_{out}(i)\mu_{\min}^2}{4}\right)$$

Bounding misclassification rate. For a labeling $e : v(\mathbf{y}) \rightarrow [K]$, the misclassification rate is

$$M_{v(\mathbf{y})}(e) = \inf_{\rho' : [K] \rightarrow [K]} \frac{1}{v(\mathbf{y})} \sum_{i=1}^{v(\mathbf{y})} 1[\hat{B}(i) = \rho' B(i)]$$

where $\hat{B}(i) = e(i)$. Let $N(\xi(e)) = \sum_{i=1}^{v(\mathbf{y})} 1(\epsilon_{out,i} \geq 0)$. Then the misspecification rate is bounded by :

$$M_{v(\mathbf{y})}(e) \leq \frac{N(\xi(e))}{v(\mathbf{y})} \quad (5)$$

The inequality is due to treating the ambiguous case $\epsilon_{out,i} = 0$ as an error. Note that we prove the case for a specific labeling e rather than an arbitrary labeling e that satisfying Assumption A.2. It is sufficient to show the RHS of inequality (5) is bounded. Lemma A.4 shows that the RHS converges almost surely to

Lemma A.4. *Given the out degree sequence $\{Deg_{out}(i)\}_{i \in v(\mathbf{y})}$ and propensities $\{f_j^{(b)}\}$ generated via the B-VCM, then*

$$P_{out} := \frac{1}{v(\mathbf{y})} \sum_{i=1}^{v(\mathbf{y})} P(\epsilon_{out,i} > 0) \xrightarrow{a.s.} \sum_{d=1}^{\infty} \alpha B(d, \alpha + 1) \exp(-d\mu_{\min}^2/4)$$

Proof. Let $P_{out} = \frac{1}{v(\mathbf{y}_1)} \sum_{i=1}^{v(\mathbf{y}_1)} P(\epsilon_{out,i} > 0)$. The RHS can be rewritten as $\sum_{d=1}^{\infty} p_d \exp(-\frac{d(\mu_{\min})^2}{4})$, where d is the degree, and p_d is the fraction of the nodes with degree d . By Theorem 2.11, $p_d \xrightarrow{a.s.} \alpha B(d, \alpha + 1)$, i.e., the degree distribution converges almost surely to the Yule-Simon Distribution. The conclusion follows immediately. \square

Bounding the RHS of (5) . We next show $\frac{1}{v(\mathbf{y})}N(\xi(e))$ is bounded. The proof relies on the following Lemma 5 from [amini2013pseudo] which we write here for convenience:

Lemma A.5. *For independent Bernoulli R.V. X_i , $i \in [n]$ and any $u > \frac{1}{e}$,*

$$P\left(\bar{X} \geq eu \frac{1}{n} \sum_{i=1}^n \mathbb{E}(X_i)\right) \leq \exp\left(-e \left(\sum_{i=1}^n \mathbb{E}(X_i)\right) u \log u\right)$$

Note that $1(\epsilon_{out,i} \geq 0)$ is a Bernoulli random variable. Given $\{f_i^{(b)}\}$, $1(\epsilon_{out,i} > 0)$ are independent random variables for $i \in [v(\mathbf{y})]$. Then by Lemma A.5:

$$P\left[\frac{1}{v(\mathbf{y})}N(\xi(e)) \geq euP_{out}\right] \leq \exp(-ev(\mathbf{y})P_{out}u \log u)$$

which guarantees that as $m \rightarrow \infty$ the misclassification rate can be bounded by $u \cdot e \cdot P_{out}$. By Lemma A.4, P_{out} converges to a constant. We next restrict to higher-degree nodes which allows us to have the misclassification rate go to zero as $m \rightarrow \infty$.

Lemma A.6. *Let $v_D(\mathbf{y})$ denote the set of nodes with degree greater than D . Then define*

$$P_D = \frac{1}{v_D(\mathbf{y})} \sum_{i=1}^{v_D(\mathbf{y})} P(\epsilon_{out,i} > 0) \rightarrow C_\alpha^{-1} \sum_{d>D} \alpha B(d, \alpha + 1) \exp(-d\mu_{min}^2/4)$$

where $C_\alpha = \sum_{d>D} \alpha B(d, \alpha + 1) \leq 1$. Then one can construct a sequence D_m , such that as $m(\mathbf{y}) \rightarrow \infty$, $P_{D_m} \rightarrow 0$, and $v_{D_m}(\mathbf{y})P_{D_m} \rightarrow \infty$. Any such sequence guarantees

$$\lim_{m(\mathbf{y}) \rightarrow \infty} P\left(\frac{1}{v_{D_m}(\mathbf{y})} N_{D_m}(\xi(e_{out})) > 0\right) = 0.$$

Figure 1 plots the P_{D_m} and $v_{D_m}(\mathbf{y})P_{D_m}$ as a function of the degree cutoff when $D = \log(m(\mathbf{y}))$.

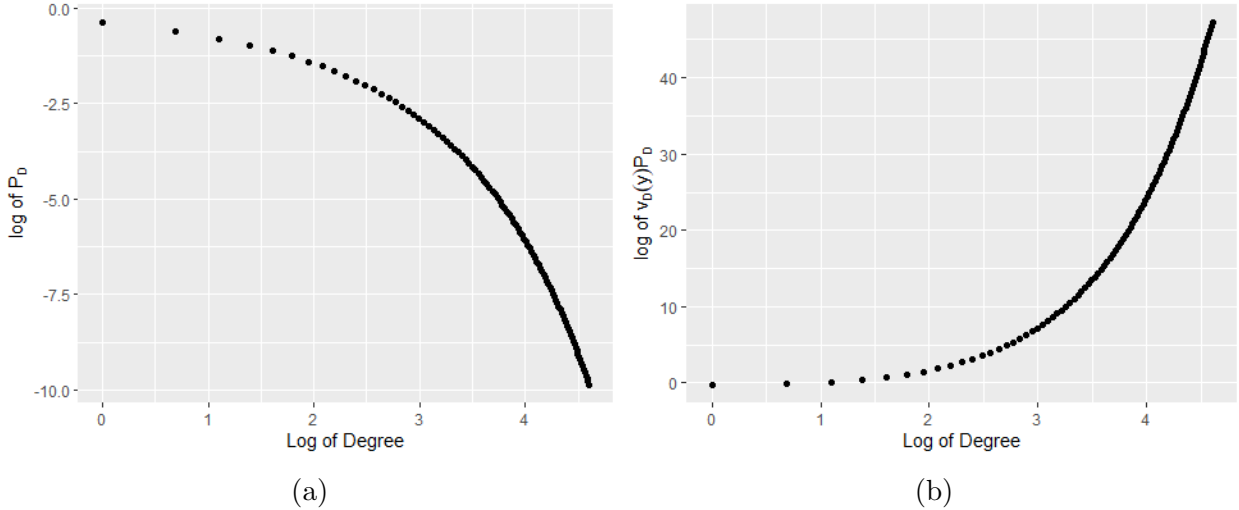


Figure 1: (a) P_{D_m} as a function of the degree cutoff; (b) $v_{D_m}(\mathbf{y})P_{D_m}$ as a function of the degree cutoff. P_{D_m} is approximated by $C_\alpha^{-1} \sum_{d>D_m} \alpha B(d, \alpha + 1) \exp(-d\mu_{min}^2/4)$, and $v_{D_m}(\mathbf{y})$ is approximated by $v(\mathbf{y}) \cdot D_m B(D_m, \alpha + 1)$ by applying Yule's law. The $v(\mathbf{y})$ is approximated by $m(\mathbf{y})^\alpha$. Specifically, $D_m = \log(m(\mathbf{y}))$, which leads to $v_{D_m}(\mathbf{y}) \simeq \exp(D_m)^\alpha D_m B(D_m, \alpha + 1)$.

From Directed to the Undirected Setting. By symmetry we have the same bound for the mis-specification rate of the nodes when considering the in-degree of the nodes. The reason we needed to prove these bounds separately is that the concentration inequalities can only be applied to *independent* random variables. When considering the total degree of each node, the same interaction impacts out- and in-degree of the two nodes involved in the interaction. Therefore, the independence assumption is violated. To overcome this, we show how to use these separate in- and out- misspecification bounds to bound the misspecification in the undirected case.

Here, we consider the degree of the complete network. We define ϵ_i in a similar way as we did in the directed case. The misclassification of the node can happen only if the node is misclassified either in out-degree or in-degree. In other words, $1(\epsilon_i > 0) \leq 1(\epsilon_{out,i} > 0) + 1(\epsilon_{in,i} > 0)$.

Note that in the presence of self interaction loop, we can rewrite $\epsilon_i = 2 * \epsilon_{self,i} + \epsilon_{out,-i} + \epsilon_{in,-i}$. A node is mis-classified if it is mis-labelled in either e_{out} or e_{in} , or it is mis-classified given the in degree or out degree. In other words, $1(\epsilon_i > 0) \leq 1(\epsilon_{self,i} > 0) + 1(\epsilon_{out,-i} > 0) + 1(\epsilon_{in,-i} > 0)$. This is bounded by $1(\epsilon_{out,i} > 0) + 1(\epsilon_{in,i} > 0)$.

With this in mind, we can take the average sum of all the nodes in the network, which gives:

$$\frac{1}{v(\mathbf{y})}N(\xi(e)) \leq \frac{1}{v(\mathbf{y})}N(\xi(e_{out})) + \frac{1}{v(\mathbf{y})}N(\xi(e_{in}))$$

which leads to:

$$\begin{aligned} P\left(\frac{1}{v(\mathbf{y})}N(\xi(e))\right) &\geq euP_{out} + euP_{in} \\ &\leq \exp(-ev(\mathbf{y})P_{out}u \log u) + \exp(-ev(\mathbf{y})P_{in}u \log u) \end{aligned}$$

Follow a similar arguments as shown before, we can get to the conclusion that for high

degree nodes in the network considering both in and out degree:

$$\lim_{m(\mathbf{y}) \rightarrow \infty} P \left(\frac{1}{v_{D_m}(y_m)} N_{D_m}(\xi(e)) > 0 \right) = 0$$

A.2 Proof of Theorem 2.9

Let \mathbf{Y}_m be an interaction network consisting of m interactions generated by the sequential description from Section 2.4. Let $v(\mathbf{Y}_m)$ be the number of vertices in the network. Within each community, denote $v^{(b)}(\mathbf{Y}_m)$, $b \in [K]$ as the number of nodes in b th sub-network. Recall the block-specific parameters $0 < \alpha_b < 1$, and $\theta_b > -\alpha_b$. Since each block-specific sub-network is generated following an equivalent sequential description as the Hollywood model, the first half of Theorem 2.9 follows by Theorem 4.3 in [crane2016edge]. Specifically, by Theorem 3.8 in [pitman2002combinatorial] we have

$$\mathbb{E}(v^{(b)}(\mathbf{Y}_m)) \sim \frac{\Gamma(\theta_b + 1)}{\alpha_b \Gamma(\theta_b + \alpha_b)} (\mu_b m)^{\alpha_b}, \quad n \rightarrow \infty$$

for $b \in [K]$, where $a_n \sim b_n$ for two sequences a_n and b_n implies $a_n/b_n \rightarrow 1$ as $n \rightarrow \infty$, and μ_b is the average arity of interactions when restricting to nodes from block b .

We can express the arity μ_b in terms of the within- and between-block propensities $\{\mathcal{B}(b, b')\}_{b, b' \in [K]}$ and probabilities of initiating an interaction $\{\pi_b\}_{b \in [K]}$ so the above statement can be re-expressed as

$$\mathbb{E}(v^{(b)}(\mathbf{Y}_m)) \sim \frac{\Gamma(\theta_b + 1)}{\alpha_b \Gamma(\theta_b + \alpha_b)} \left[m \times \left(\pi_b + \sum_{k=1}^{\infty} \nu_k \sum_{b'} \pi_{b'} k \mathcal{B}(b', b) \right) \right]^{\alpha_b}$$

where ν_k is the distribution over the number of commentators (e.g, $\nu_1 = 1$ is the simple case of a single commentator in every interaction). By linearity of expectations we then have:

$$\mathbb{E}(v(\mathbf{Y}_m)) = \sum_b \mathbb{E}(v^{(b)}(\mathbf{Y}_m)) \sim \sum_b \frac{\Gamma(\theta_b + 1)}{\alpha_b \Gamma(\theta_b + \alpha_b)} \left[m \times \left(\pi_b + (\mu - 1) \sum_{b'} \pi_{b'} \mathcal{B}(b', b) \right) \right]^{\alpha_b}$$

where $\mu = 1 + \sum_{k \geq 1} k\nu_k$ is the average global arity.

To establish global sparsity of $(\mathbf{Y}_m)_{m \geq 1}$, consider $(m^{-1}v(\mathbf{Y}_m)^{m \bullet (\mathbf{Y}_m)})$ where $m \bullet (\mathbf{Y}_m)$ is the average total degree of \mathbf{Y}_m . By the strong law of large numbers, $m \bullet (\mathbf{Y}_m) \rightarrow \mu$ a.s. as $m \rightarrow \infty$ where $\mu = 1 + \sum_{k \geq 1} \nu_k k$ is the average arity of an interaction. Let $\alpha_\star = \max_b \alpha_b$, and b_\star indicate the corresponding block. By the above discussion, $v(\mathbf{Y}_m) \sim (\mu m)^{\alpha_\star} S$ a.s. as $m \rightarrow \infty$ for a strictly positive and finite random variable S . It follows that $m^{-1}v(\mathbf{Y}_m)^{m \bullet (\mathbf{Y}_m)} \sim m^{-1}(\mu m)^{\mu \alpha_\star} S$ a.s. as $m \rightarrow \infty$ which goes to infinity as long as $\mu \alpha_\star > 1$. Thus, (\mathbf{Y}_m) is sparse with probability 1 provided $1/\mu < \alpha_\star < 1$.

A.3 Proof of Theorem 2.11

Let \mathbf{Y}_m be an interaction network consisting of m interactions generated by the sequential description from Section 2.4. Let $v(\mathbf{Y}_m)$ be the number of vertices in the network. Within each community, denote $v^{(b)}(\mathbf{Y}_m)$, $b \in [K]$ as the number of nodes in b th sub-network. Recall the block-specific parameters $0 < \alpha_b < 1$, and $\theta_b > -\alpha_b$. Since each block-specific sub-network is generated following an equivalent sequential description as the Hollywood model, the first half of Theorem 2.11 follows by Theorem 4.2 in [crane2016edge]. Specifically, by Theorem 3.11 in [pitman2002combinatorial] we have $N_d^{(b)}(\mathbf{Y}_m)/v^{(b)}(\mathbf{Y}_m) \rightarrow \alpha_b B(d, \alpha_b + 1)$ a.s. for every $d \geq 1$ as $m \rightarrow \infty$.

To prove global power-law, we note that $N_d(\mathbf{Y}_m) = \sum_{b=1}^K N_d^{(b)}(\mathbf{Y}_m)$, then $N_d(\mathbf{Y}_m)/v(\mathbf{Y}_m) = \sum_b N_d^{(b)}(\mathbf{Y}_m)/v^{(b)}(\mathbf{Y}_m) \cdot v^{(b)}(\mathbf{Y}_m)/v(\mathbf{Y}_m) \rightarrow \alpha_{b_\star} B(d, \alpha_{b_\star} + 1)$ since $v^{(b)}(\mathbf{Y}_m)/v(\mathbf{Y}_m) \rightarrow 1[\alpha_b = \alpha_{b_\star}]$ a.s. as $m \rightarrow \infty$.

A.4 Proof of Theorem 2.5

We prove here a general characterization of edge exchangeable networks with node-level community structure with undirected binary edges. Let $\text{fin}_2(\mathcal{P})$ denote the set of all multisets of size 2. We assume $\mathcal{P} = \mathbb{N}$, i.e., the population is countably infinite. The directed and multiple arity edge cases follows a similar argument with some additional notation.

Given a binary interaction-labelled network \mathbf{Y} with $e(\mathbf{Y}) = n$, let $S : [n] \rightarrow \text{fin}_2(\mathbb{N})$ denote a *selection function for \mathbf{Y}* if S is an interaction process whose induced interaction-labelled network agrees with \mathbf{Y} . Let $S_B[n] \rightarrow \text{fin}_2([K])$ denote the *block selection function for \mathbf{Y}* which induces the block network from \mathbf{Y} . For simplicity, we say selection function to refer to the pair $\mathbf{S} := (S, S_B)$ since the two jointly define an interaction-labelled network with block structure. Two selection functions \mathbf{S}, \mathbf{S}' are equivalent, $\mathbf{S} \equiv \mathbf{S}'$, if they correspond to the same interaction-labelled network with the same block structure. To every interaction-labelled network with block structure, we associate a canonical selection function defined by labeling the vertices *and the blocks* in order of appearance.

The $\text{fin}_2([K] \times \mathbb{N})$ simplex consists of all $(f_{(b,i),(b',j)})$ such that for all $j, i \geq -1$ $f_{(b,-1),(b',i)} = 0$ for all $b, b' \in [K]$ and $i \neq 0$, and $\sum_{b,b' \in [K], i, j \geq -1} f_{(b,i),(b',j)} = 1$. For any f in the simplex and $b \in [K]$ define

$$f_{\bullet}^{(b)} = \sum_{i, j \geq -1, b' \in [K]} f_{(b,i),(b',j)}$$

$$f_{\bullet}^{(b,i)} = \sum_{j \geq -1, b' \in [K]} f_{(b,i),(b',j)}.$$

Every $f = (f_{(b,i),(b',j)})_{i, j \geq -1, b, b' \in [K]}$ in the joint $\text{fin}_2([K] \times \mathbb{N})$ simplex determines a probability distribution on interaction-labelled networks with block structure, denoted ϵ_f , as follows. Let E_1, E_2, \dots be random iid random pairs $\{(b, i), (b', j)\}$ with

$$P(E_i = \{(b, i), (b', j)\} | f) = f_{\{(b,i),(b',j)\}}, \quad j, i \geq -1 \quad \text{and} \quad b, b' \in [K] \quad (6)$$

Given the sequence E_1, E_2, \dots we define the selection function $S : \mathbb{N} \rightarrow \text{fin}_2([K] \times \mathbb{Z})$ as follows. Let $m_{0,b} = 0$ for each $b \in [K]$. For $n \geq 1$, suppose $m_{n-1,b} = z_b \leq 0$ for each $b \in [K]$. If E_n contains no 0s, then $S(n) = E_n$ and $m_{n,b} = m_{n-1,b}$. If $E_n = \{(b, 0), (b', j)\}$ for some $j \geq 1$ then $S(n) = \{(b, z_b - 1), (b', j)\}$ and update $m_{n,b} = z_b - 1$. If $E_n = \{(b, 0), (b', 0)\}$ then $S(n) = \{(b, z_b - 1), (b', z_{b'} - 1)\}$ and update $m_{n,b} = z_b - 1$ and $m_{n,b'} = z_{b'} - 1$. If $E_n =$

$\{(b, 0), (b, 0)\}$ then $S(n) = \{(b, z_b - 1), (b, z_b - 1)\}$ and $m_{n,b} = z_b - 1$. If $E_n = \{(b, 0), (b, -1)\}$ then $S(n) = \{(b, z_b - 1), (b, z_b - 2)\}$ and $m_{n,b} = z_b - 2$. These events are ‘blips’ that involve vertices in different blocks that appear once and never again. Define \mathbf{Y}_B to be the interaction-labelled network with block structure B induced by S .

Proposition A.7. *The block-labelled network \mathbf{Y}_B corresponding to E_1, E_2, \dots iid from (6) is block interaction exchangeable for all f in the $\text{fin}_2([K] \times [N])$ -simplex.*

For identifiability, we define the *rank ordering* of f by $f^\downarrow = \left(f_{\{(b,i),(b',j)\}}^\downarrow \right)$ which is obtained by first reordering blocks $1, \dots, K$ so that $f_{\bullet}^{(b)} \geq f_{\bullet}^{(b')}$ for all $b' > b$. Then we reorder elements within each block $1, 2, \dots$ so that $f_{\bullet}^{(b,i)} \geq f_{\bullet}^{(b,i+1)}$ for $i \geq 1$. Ties can be handled in a similar fashion as in [crane2016edge]. Write \mathcal{F}^\downarrow to denote the space of rank reordered elements of the $\text{fin}_2([K] \times \mathbb{N})$ -simplex.

As vertex labels other than -1 and 0 are inconsequential, ϵ_f and $\epsilon_{f'}$ determine the same distribution for any f, f' for which $f^\downarrow = f'^\downarrow$. For any edge-labeled network \mathbf{Y} , then $|\mathbf{Y}|^\downarrow \in \mathcal{F}^\downarrow$ denote its signature, if it exists, as follows. Let $S_{\mathbf{Y}}$ be the canonical selection function for \mathbf{Y} . For every $\{(b, i), (b', j)\}$ $j \geq i \geq 1$ define

$$\begin{aligned} f_{\{(b,i),(b',j)\}}(\mathbf{Y}) &= \lim_{n \rightarrow \infty} n^{-1} \sum_{k=1}^n 1[S_{\mathbf{Y}}(k) = \{(b, i), (b', j)\}] \\ f_{\bullet}^{(b,b')}(\mathbf{Y}) &= \lim_{n \rightarrow \infty} n^{-1} \sum_{k=1}^n 1[(b, b') \in S_{\mathbf{Y}}(k)] \\ f_{\bullet}^{(b,(b',j))}(\mathbf{Y}) &= \lim_{n \rightarrow \infty} n^{-1} \sum_{k=1}^n 1[(b, (b', j)) \in S_{\mathbf{Y}}(k)] \\ f_{\bullet}^{(i,j)}(\mathbf{Y}) &= \lim_{n \rightarrow \infty} \frac{\sum_{k=1}^n 1[S_{\mathbf{Y}}(k) = \{(b, i), (b', j)\}]}{\sum_{k=1}^n 1[(b, b') \in S_{\mathbf{Y}}(k)]}. \end{aligned}$$

if the limits exist, where $f_{\bullet}^{(i,j)}(\mathbf{Y})$ implicitly depends on (b, b') , i.e., it is the asymptotic

fraction of interactions between b and b' that include i and j . We also define

$$\begin{aligned}
f_{\{(b,0),(b',j)\}}(\mathbf{Y}) &= f_{\bullet}^{(b,(b',j))}(\mathbf{Y}) - \sum_{i=1}^{\infty} f_{\{(b,i),(b',j)\}}(\mathbf{Y}) \\
f_{\{(b,0),(b',0)\}}(\mathbf{Y}) &= f_{\bullet}^{(b,b')}(\mathbf{Y}) - \sum_{i,j=1}^{\infty} f_{\{(b,i),(b',j)\}}(\mathbf{Y}) \\
f_{\{(b,0),(b,0)\}}(\mathbf{Y}) &= \lim_{n \rightarrow \infty} n^{-1} \sum_{k=1}^n \left(\sum_{l \geq 1} 1 [\{(b,l),(b,l)\} = S_{\mathbf{Y}}(k)] \right) - \sum_{i=1}^{\infty} f_{\{(b,i),(b,i)\}}(\mathbf{Y}) \\
f_{\{(b,-1),(b,0)\}}(\mathbf{Y}) &= \lim_{n \rightarrow \infty} n^{-1} \sum_{k=1}^n \left(\sum_{l,r \geq 1; l \neq r} 1 [\{(b,l),(b,r)\} = S_{\mathbf{Y}}(k)] \right) - \sum_{j > i \geq 1}^{\infty} f_{\{(b,i),(b,j)\}}(\mathbf{Y}).
\end{aligned}$$

We can similarly define $f_{\bullet}^{(0,j)}(\mathbf{Y})$ and other blip terms that are specific to pairs (b, b') as above.

Theorem A.8. *Let \mathbf{Y} be an interaction exchangeable network with block structure. Then there exists a unique probability measure on $\phi = (\phi_K, \{\phi_{\bar{b}}\})$ on \mathcal{F}^{\downarrow} such that $\mathbf{Y} \sim \epsilon_{\phi}$, where*

$$\epsilon_{\phi} = \int_{\mathcal{F}^{\downarrow}} \epsilon_f(\cdot) \phi(df) \quad (7)$$

That is, every interaction exchangeable network with block structure B can be generated by first sampling $f_K \sim \phi_K$ then sampling $\{\phi_{\bar{b}}\} \sim \phi_{\bar{b}}$ and then, given $f := (f_k, \{\phi_{\bar{b}}\})$, generating the interaction process according to (6).

Theorem 2.5 follows as a corollary to Theorem A.8 by ruling out blips.

Proof of Theorem A.8. Equip the space of interaction labelled networks with block structure with the product-discrete topology induced by the metric

$$d(\mathbf{Y}, \mathbf{Y}') = (1 + \sup\{n \in \mathbb{N} : \mathbf{Y}_n = \mathbf{Y}'_n\})^{-1}$$

with $1/\infty = 0$, and \mathcal{F}^\downarrow with the topology induced by

$$d_{\mathcal{F}^\downarrow}(f, f') = \sum_{b, b'} \sum_{j \geq i \geq -1} |f_{\{(b, i), (b', j)\}} - f'_{\{(b, i), (b', j)\}}|$$

We work with the Borel σ -fields induced by these topologies.

Let \mathbf{Y} be an interaction exchangeable random network with block structure B . Let $S_{\mathbf{Y}}$ be the canonical selection function, and (ξ_1, \dots, ξ_K) and $\xi_1^{(b)}, \xi_2^{(b)}, \dots$ for each $b \in [K]$ be K iid sequences of $\text{Uniform}[0, 1]$ random variables, which are independent of \mathbf{Y} . Given \mathbf{Y} and $\xi := \left(\{\xi_k\}_{k=1}^K, \{\xi_i^{(b)}\}_{i \geq 1, b \in [K]} \right)$, we define $Z : \mathbb{N} \rightarrow \text{fin}_2([0, 1] \times [0, 1])$ by $Z(n) = \{(\xi_b, \xi_i^{(b)}), (\xi_{b'}, \xi_j^{(b')})\}$ on the event $S_{\mathbf{Y}}(n) = \{(b, i), (b', j)\}$ for $n \geq 1$.

By independence of \mathbf{Y} and ξ and interaction exchangeability of \mathbf{Y} , $(Z(n))_{n \geq 1}$ is an exchangeable sequence taking values in the Polish space $\text{fin}_2([0, 1] \times [0, 1])$. By de Finetti's theorem, there exists a unique measure μ on the space of probability measures on $\text{fin}_2([0, 1] \times [0, 1])$ such that $Z =_D Z^* = (Z^*(n))_{n \geq 1}$ with

$$pr(Z^* \in \cdot) = \int m^\infty(\cdot) \mu(dm),$$

where m^∞ denotes the infinite produce measure of m . Specifically there exists a random measure ν on $\text{fin}_2([0, 1] \times [0, 1])$ such that $P(Z \in \cdot | \nu) = \nu^\infty$ almost surely. Given ν , we define

$$\begin{aligned} f_{\{(b, i), (b', j)\}} &= \nu(\{(\xi_b, \xi_i^{(b)}), (\xi_{b'}, \xi_j^{(b')})\}), \quad i, j \geq 1 \\ f_{\bullet}^{(b, b')} &= \nu(\{(x_1, y_1), (x_2, y_2)\} \in \text{fin}_2([0, 1] \times [0, 1]) : (\xi_b, \xi_{b'}) = \{x_1, x_2\}), \\ f_{\bullet}^{\{(b, i), (b', j)\}} &= \nu(\{(x_1, y_1), (x_2, y_2)\} \in \text{fin}_2([0, 1] \times [0, 1]) : (\xi_b, \xi_{b'}) = \{x_1, x_2\}, \xi_j^{(b')} \in (y_1, y_2)), \\ f_{\bullet}^{(i, j)} &= f_{\{(b, i), (b', j)\}} / f_{\bullet}^{(b, b')}, \end{aligned}$$

and the blip-related terms:

$$\begin{aligned}
f_{\{(b,0),(b',j)\}} &= f_{\bullet}^{\{(b,(b',j))\}} - \sum_{i=1}^{\infty} f_{\{(b,i),(b,j)\}} \\
f_{\{(b,0),(b',0)\}} &= f_{\bullet}^{\{(b,b')\}} - \sum_{i,j=1}^{\infty} f_{\{(b,i),(b',j)\}} \\
f_{\{(b,0),(b,0)\}} &= \nu \left(\{(x_1, y_1), (x_2, y_2)\} \in \text{fin}_2([0, 1] \times [0, 1]) : \right. \\
&\quad \left. (\xi_b, \xi_b) = \{x_1, x_2\}, \{u, u\} \in \{y_1, y_2\} \right) - \sum_{i=1}^{\infty} f_{\{(b,i),(b,i)\}} \\
f_{\{(b,0),(b,-1)\}} &= \nu \left(\{(x_1, y_1), (x_2, y_2)\} \in \text{fin}_2([0, 1] \times [0, 1]) : \right. \\
&\quad \left. (\xi_b, \xi_b) = \{x_1, x_2\}, \{u, v\} \in \{y_1, y_2\}, u \neq v \right) - \sum_{j>i \geq 1}^{\infty} f_{\{(b,i),(b,j)\}}.
\end{aligned}$$

We can then define blip-related terms, e.g., $f^{(0,j)} = f_{\{(b,0),(b',j)\}} / f_{\bullet}^{\{(b,b')\}}$, in a similar fashion.

By construction $(f_{\{(b,i),(b',j)\}})$ is in the $\text{fin}_2([K] \times \mathbb{N})$ -simplex and therefore, $f^{\downarrow} \in \mathcal{F}^{\downarrow}$. Given ν , let (Z', S') be an iid copy of $(Z, S_{\mathbf{Y}})$ and let \mathbf{Y}' be the interaction-labelled network induced by S' . We next show that $\text{pr}(\mathbf{Y}' \in \cdot | \nu) = \epsilon_{f^{\downarrow}}$ for f^{\downarrow} defined above from ν .

Define $A_{b,b'} := \{(i, j) \in \mathbb{N}^2 : f_{\bullet}^{\{(i,j)\}} > 0\}$ and $\xi_{A_{b,b'}} := \{(\xi_i^b, \xi_j^{b'}) : (i, j) \in A_{b,b'}\}$. Then it follows that

$$\text{pr}(Z'(1) \cap \xi_{A_{b,b'}} = \emptyset | \nu, (b, b') \in Z'(1)) = f_{\{(b,0),(b',0)\}} + 1[b = b'] f_{\{(b,0),(b,-1)\}}.$$

and

$$\text{pr}(Z'(1) \cap \xi_{A_{b,b'}} = \{i\} | \nu, (b, b') \in Z'(1)) = f_{\{(b,i),(b',0)\}}$$

By exchangeability, $(i, j) \notin A_{b,b'}$ implies $\{(\xi_b, \xi_i^{(b)}), (\xi_{b'}, \xi_j^{(b')})\}$ appears at most once in Z with

probability 1. Moreover,

$$\text{pr}(Z'(1) \cap \{(b, \xi_{A_b, b})\} = \emptyset \text{ and } Z'_B(1) = \{(b, u), (b, u)\} \text{ for some } u \in [0, 1] | \nu) = f_{\{(b, 0), (b, 0)\}},$$

$$\text{pr}(Z'(1) \cap \{(b, \xi_{A_b, b})\} = \emptyset \text{ and } Z'_B(1) = \{(b, u), (b, v)\} \text{ for some } u \neq v \in [0, 1] | \nu) = f_{\{(b, 0), (b, -1)\}},$$

Now define $X' : \mathbb{N} \rightarrow \text{fin}_2([K] \times \mathbb{N} \cup \{-1, 0\})$ and the random selection function $S_{X'}$ as follows.

Let $m_0^{(b)} = 0$ for all $b \in [K]$. For $n \geq 1$, suppose $m_{n-1}^{(b)} = z_b \leq 0$. If $Z'(n) \cup \xi_{A_b} = \{\xi_i\}$ and $Z'(n) \cup \xi_{A_{b'}} = \{\xi_j\}$ for some $i, j \in \mathbb{N}$ and $b, b' \in [K]$ then put $X'(n) = S_{X'}(n) = \{(b, i), (b', j)\}$.

If $(b, b') \in Z'(n)$ with $b \neq b' \in [K]$ and $Z'(n) \cup \xi_{A_b} = \emptyset$ but $Z'(n) \cup \xi_{A_{b'}} = \{\xi_j\}$ then put $X'(n) = S_{X'}(n) = \{(b, z_b - 1), (b', j)\}$ and set $m_n^{(b)} = z_b - 1$.

If $(b, b) \in Z'(n)$ and $Z'(n) \cup \xi_{A_b} = \emptyset$ and $Z'(n) = \{(b, u), (b, u)\}$ for some $u \in [0, 1]$ then put $X'(n) = S_{X'}(n) = \{(b, z_b - 1), (b, z_b - 1)\}$ and set $m_n^{(b)} = z_b - 1$.

If $(b, b) \in Z'(n)$ and $Z'(n) \cup \xi_{A_b} = \emptyset$ and $Z'(n) = \{(b, u), (b, v)\}$ for some $u \neq v \in [0, 1]$ then put $X'(n) = S_{X'}(n) = \{(b, z_b - 1), (b, z_b - 2)\}$ and set $m_n^{(b)} = z_b - 2$.

By construction, $S_{X'} \equiv S'$ and, given f , X' is conditionally i.i.d from (6).

The integral representation in (7) follows by de Finetti's theorem, which completes the proof. \square

A.5 Misspecification Rate as a function of degree cutoff

Section 4.0.1 showed the L_2 norm as a function of the degree cutoff where the inferred block assignments are calculated based on the average block assignments over the Gibbs samplers. Here, we consider another criteria to assess the inferred block assignments that is based on the mis-specification rate defined as $\inf_{\rho: [K] \rightarrow [K]} \frac{1}{v(\mathbf{y}_m)} \sum_{i=1}^{v(\mathbf{y}_m)} \mathbf{1}(\mathcal{B}(i) \neq \rho \hat{\mathcal{B}}(i))$. A binary classifier $\hat{\mathcal{B}}(i)$ for each node is determined by whether the node has more than 0.5 of chance being assigned to a certain block in all valid Gibbs iterations. The results are shown in Figure 2. The conclusions are similar to the conclusions in Section 4.0.1, where the misspecification rate decreases to 0 as increase of the degree cutoff.

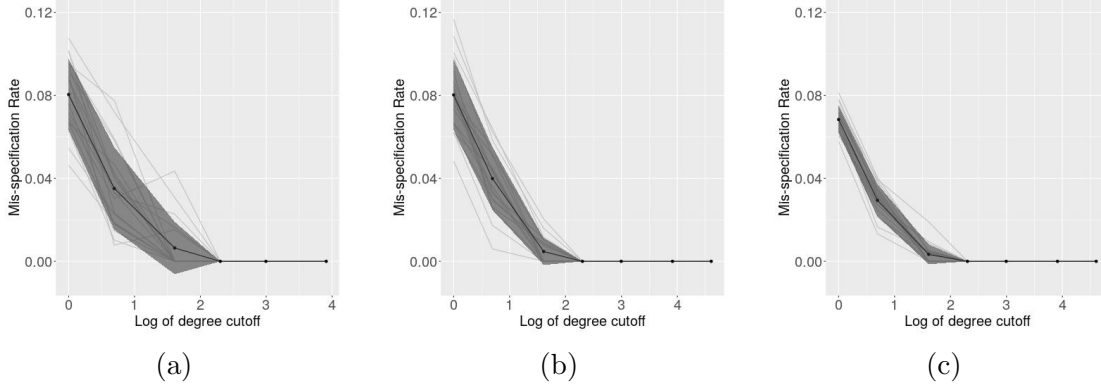


Figure 2: The mis-specification rate as a function of the degree cutoff, in the setting where $\alpha_1 = \alpha_2 = 0.5$, $\mathcal{B}(1, 1) = \mathcal{B}(2, 2) = 0.9$, with (a) 1,000, (b) 2,500, and (c) 10,000 interactions presented in the network. The solid dark line is the average L_2 norm over 20 repeats. The L_2 norm is calculated based on a binary classifier for each node.

A.6 L_2 norm for high-degree nodes

To demonstrate the consistency conclusion on high-degree nodes, we calculate the L_2 norm for nodes with degree greater than certain threshold. We select the cutoff value at $0.1 * m(\mathbf{y}_m)^\alpha$. The multiplication of constant 0.1 is to guarantee the existence of nodes with degree greater than the cutoff value, especially when α is large. The results are shown in Table 1. A significant decrease in the L_2 norms are observed. For example, in the setting where $\alpha_1 = \alpha_2 = 0.7$, $\mathcal{B}(1, 1) = \mathcal{B}(2, 2) = 0.9$, $m(\mathbf{y}_m) = 10,000$, the L_2 norm decreases from 0.143 (0.008) to 0 (0). Note that when the power-law parameter is small, i.e. $\alpha_1 = \alpha_2 = 0.1$, the degree cutoff threshold is smaller than 1. That is, all the nodes are included when calculating the L_2 norm. Therefore, the corresponding results don't change from Table 1 in main context.

A.7 Recovering Block structure with different power-law parameter values

In Section 4, we show the results from the setting where the power-law parameters $\alpha_1 = \alpha_2$. Table 1 shows the L_2 norm calculated from two blocks of different power-law parameter values. The generative model is the same as we used in the Section 4.0.2.

	# Interactions	$\mathcal{B} = \{0.1, 0.9\}$	$\mathcal{B} = \{0.3, 0.7\}$	$\mathcal{B} = \{0.5, 0.5\}$
$\alpha = \{0.1, 0.1\}$	1,000	0.043 (0.016)	0.183 (0.033)	0.458 (0.028)
	2,500	0.067 (0.096)	0.161 (0.042)	0.457 (0.023)
	10,000	0.053 (0.072)	0.23 (0.14)	0.454 (0.018)
$\alpha = \{0.3, 0.3\}$	1,000	0.075 (0.013)	0.255 (0.067)	0.475 (0.020)
	2,500	0.024 (0.009)	0.162 (0.072)	0.461 (0.035)
	10,000	0.019 (0.006)	0.166 (0.090)	0.459 (0.026)
$\alpha = \{0.5, 0.5\}$	1,000	0.010 (0.006)	0.131 (0.028)	0.454 (0.038)
	2,500	0.002 (0.003)	0.087 (0.081)	0.463 (0.027)
	10,000	3.76e-6 (6.59e-6)	0.055 (0.084)	0.460 (0.017)
$\alpha = \{0.7, 0.7\}$	1,000	0.022 (0.092)	0.091 (0.099)	0.457 (0.031)
	2,500	0 (0)	0.042 (0.064)	0.455 (0.026)
	10,000	0 (0)	3.44e-6 (1.14e-5)	0.433 (0.027)
$\alpha = \{0.9, 0.9\}$	1,000	0.074 (0.155)	0.314 (0.157)	0.360 (0.128)
	2,500	0.007 (0.030)	0.099 (0.153)	0.308 (0.143)
	10,000	0 (0)	0.056 (0.101)	0.171 (0.131)

Table 1: Standardized average L2 norm (SD) of the inferred block assignments and the underlying truth for high-degree nodes with the degree cutoff set to be proportional to $m(\mathbf{y}_m)$.

From the results shown in Table 1, we get the following conclusions. First, for fixed $\{\alpha_1, \alpha_2\}$, the higher the within block connection probability, the better the recovery of the block assignments. Second, as the number of observations increases, accuracy of the inferred block assignments increases across almost all settings. Third, for fixed \mathcal{B} as the difference in power-law parameters decreases between the two blocks, the block assignment accuracy decreases.

A.8 Cross Entropy Loss

In Section 4.0.1, the L_2 norm was used as one metric to check if inferred block assignment agrees with the true block assignments (up to label switching). Here, we show another metric that can be applied to $K > 2$ scenarios. The *cross entropy loss* is defined for a specific block

	Interactions	$\alpha = \{0.1, 0.9\}$	$\alpha = \{0.2, 0.8\}$	$\alpha = \{0.3, 0.7\}$	$\alpha = \{0.4, 0.6\}$
$\mathcal{B} = \{0.1, 0.9\}$	1,000	0.085 (0.049)	0.111 (0.070)	0.151 (0.077)	0.172 (0.079)
	10,000	0.043 (0.024)	0.047 (0.038)	0.081 (0.064)	0.151 (0.079)
	100,000	0.014 (0.011)	0.030 (0.026)	0.084 (0.056)	0.109 (0.068)
$\mathcal{B} = \{0.2, 0.8\}$	1,000	0.134 (0.031)	0.161 (0.063)	0.200 (0.086)	0.270 (0.085)
	10,000	0.061 (0.009)	0.111 (0.017)	0.202 (0.049)	0.304 (0.040)
	100,000	0.035 (0.029)	0.061 (0.007)	0.144 (0.012)	0.259 (0.020)
$\mathcal{B} = \{0.3, 0.7\}$	1,000	0.132 (0.054)	0.153 (0.071)	0.250 (0.115)	0.304 (0.076)
	10,000	0.102 (0.110)	0.092 (0.059)	0.159 (0.097)	0.271 (0.106)
	100,000	0.041 (0.076)	0.075 (0.053)	0.093 (0.054)	0.276 (0.096)
$\mathcal{B} = \{0.4, 0.6\}$	1,000	0.256 (0.094)	0.255 (0.105)	0.345 (0.089)	0.446 (0.054)
	10,000	0.187 (0.091)	0.239 (0.122)	0.275 (0.084)	0.419 (0.052)
	100,000	0.242 (0.140)	0.134 (0.084)	0.198 (0.077)	0.380 (0.073)
$\mathcal{B} = \{0.5, 0.5\}$	1,000	0.369 (0.093)	0.390 (0.078)	0.452 (0.042)	0.461 (0.042)
	10,000	0.241 (0.092)	0.261 (0.088)	0.335 (0.091)	0.451 (0.030)
	100,000	0.345 (0.067)	0.247 (0.100)	0.269 (0.112)	0.391 (0.074)

Table 2: Standardized L_2 norm of the inferred block assignments and the underlying truth in different settings. For each set with the same values of the connectivity propensity $\{a, b\}$, the power-law parameters $\{\alpha_1, \alpha_2\}$, and the number of interactions ($\{1, 000, 10, 000, 100, 000\}$), we repeated the simulation 20 times. The mean values (SD) over 20 simulations are shown here. We do observe some instability when the propensity of connection is close to 0.5.

$b \in [K]$ as:

$$\mathcal{L}_b = \sum_{j \in X_b} -p(\mathcal{B}(j) = b) \log q(\hat{\mathcal{B}}(j) = b)$$

where the $p(\cdot)$ is the probability of the true cluster assignment, and $q(\cdot)$ is the posterior mean of the inferred cluster assignment. In the two clusters scenario, for example, a node s has block labeling $\mathcal{B}(s) = 1$ in the generative model, while in the inferred block assignment, the mean probability node s being assigned to block 1 is 0.6, the cross entropy loss for node s of cluster 1 is $\mathcal{L}_s = -1 \times \log(0.6)$. In the best case where all the nodes are assigned correctly to the true block, the entropy loss is 0; in the case where the block assignments are completely wrong, the entropy loss is infinity; in the case of random guess, the expected entropy loss of a specific node is $-\log(0.5)$. Further define the overall cross entropy loss \mathcal{L} and the average per node entropy loss \mathcal{L}_s as:

$$\mathcal{L} = \sum_{b=1}^K \mathcal{L}_b; \mathcal{L}_s = \frac{1}{v(\mathbf{y}_m)} \mathcal{L}$$

The results of the per node entropy loss in the two block scenario is shown in Table 3 and Table 4. We labelled the block by selecting the smallest value of the entropy loss over all possible combinations. The results are consistent with those of the L_2 norm. Conclusions based on Table 3 and Table 4 are similar to the conclusions based on L_2 norms.

A.9 The symmetry of the propensity matrix

In the main text, we discuss the setting where the propensity matrix is not symmetric, i.e., the interaction network is directed. A natural question is “What if the interaction is not directed?” One solution is presented here.

Let $k \in [K]$ be the current dimension that’s being updated. When $k = 1$, we follow the same step as described in Section 4.2:

$$\mathcal{B}(1,) | C_m \sim \text{Dirichlet}(\nu + \vec{*})$$

	# Interactions	$\mathcal{B} = \{0.1, 0.9\}$	$\mathcal{B} = \{0.3, 0.7\}$	$\mathcal{B} = \{0.5, 0.5\}$
$\alpha = \{0.1, 0.1\}$	1,000	0.097 (0.056)	0.336 (0.075)	0.686 (0.044)
	2,500	0.143 (0.123)	0.298 (0.059)	0.665 (0.030)
	10,000	0.112 (0.121)	0.357 (0.165)	0.659 (0.028)
$\alpha = \{0.3, 0.3\}$	1,000	0.161 (0.045)	0.460 (0.114)	0.696 (0.041)
	2,500	0.143 (0.025)	0.412 (0.071)	0.465 (0.051)
	10,000	0.130 (0.027)	0.488 (0.265)	0.696 (0.040)
$\alpha = \{0.5, 0.5\}$	1,000	0.222 (0.034)	0.521 (0.028)	0.701 (0.033)
	2,500	0.223 (0.036)	0.498 (0.060)	0.703 (0.033)
	10,000	0.198 (0.016)	0.501 (0.081)	0.689 (0.026)
$\alpha = \{0.7, 0.7\}$	1,000	0.360 (0.068)	0.597 (0.034)	0.708 (0.038)
	2,500	0.318 (0.028)	0.593 (0.017)	0.694 (0.013)
	10,000	0.296 (0.017)	0.561 (0.015)	0.692 (0.026)
$\alpha = \{0.9, 0.9\}$	1,000	0.606 (0.074)	0.691 (0.016)	0.711 (0.064)
	2,500	0.550 (0.030)	0.679 (0.032)	0.696 (0.008)
	10,000	0.487 (0.032)	0.663 (0.017)	0.702 (0.013)

Table 3: Cross Entropy Loss the inferred block assignments when comparing to the underlying truth in different settings. For each set with the same values of the connectivity propensity \mathcal{B} , the power-law parameters $\{\alpha_1, \alpha_2\}$, and the number of interactions ($\{1, 000, 2, 500, 10, 000\}$), we repeated the simulation 20 times. The mean values (SD) over 20 simulations are shown here.

	Interactions	$\{\alpha_b\} = \{0.1, 0.9\}$	$\{\alpha_b\} = \{0.2, 0.8\}$	$\{\alpha_b\} = \{0.3, 0.7\}$	$\{\alpha_b\} = \{0.4, 0.6\}$
$\{a, b\} = \{0.1, 0.9\}$	1,000	0.056 (0.014)	0.095 (0.028)	0.152 (0.028)	0.212 (0.040)
	10,000	0.014 (0.004)	0.039 (0.013)	0.094 (0.012)	0.170 (0.032)
	100,000	0.0027 (0.0006)	0.013 (0.004)	0.054 (0.012)	0.134 (0.018)
$\{a, b\} = \{0.2, 0.8\}$	1,000	0.084 (0.020)	0.151 (0.032)	0.239 (0.065)	0.343 (0.050)
	10,000	0.019 (0.005)	0.055 (0.015)	0.157 (0.084)	0.298 (0.074)
	100,000	0.013 (0.033)	0.018 (0.004)	0.097 (0.040)	0.223 (0.029)
$\{a, b\} = \{0.3, 0.7\}$	1,000	0.102 (0.152)	0.182 (0.050)	0.346 (0.100)	0.445 (0.061)
	10,000	0.052 (0.118)	0.078 (0.020)	0.210 (0.089)	0.411 (0.123)
	100,000	0.039 (0.086)	0.048 (0.060)	0.099 (0.016)	0.342 (0.124)
$\{a, b\} = \{0.4, 0.6\}$	1,000	0.161 (0.082)	0.345 (0.117)	0.489 (0.097)	0.625 (0.057)
	10,000	0.120 (0.129)	0.279 (0.186)	0.311 (0.120)	0.546 (0.098)
	100,000	0.291 (0.202)	0.120 (0.125)	0.216 (0.118)	0.508 (0.103)
$\{a, b\} = \{0.5, 0.5\}$	1,000	0.311 (0.202)	0.517 (0.110)	0.621 (0.052)	0.658 (0.067)
	10,000	0.254 (0.158)	0.291 (0.140)	0.434 (0.115)	0.711 (0.136)
	100,000	0.422 (0.107)	0.283 (0.146)	0.332 (0.140)	0.604 (0.049)

Table 4: Cross Entropy Loss averaged by number of nodes in different settings. For each set with the same values of the connectivity propensity $\{a, b\}$, the power-law parameters $\{\alpha_1, \alpha_2\}$, and the number of interactions ($\{1, 000, 10, 000, 100, 000\}$), we repeated the simulation 20 times. The mean values (SD) over 20 simulations are shown here.

where the Dirichlet distribution is characterized by K parameters, $\vec{*}$ stands for the count of the interactions between block 1 and the other blocks. After the first row of the propensity matrix being sampled, we let $\mathcal{B}(, 1) = \mathcal{B}(1,)$. For an arbitrary $k \geq 2$, we follow the sequential updates as described below:

$$\mathcal{B}(k, k : K)^* | \{\mathcal{B}(1,), \dots, \mathcal{B}(k-1,)\}, C_m \sim \text{Dirichlet}(\nu_{k:K} + \vec{*}_{k:K})$$

$$\mathcal{B}(k, k : K) = \mathcal{B}(k, k : K)^* * (1 - \sum_{i=1}^{k-1} \mathcal{B}(k, i))$$

where $\nu_{k:K}$ stands for the last $K - k$ elements of the original vector ν . The notation is the same for $\vec{*}_{k:K}$ and $\vec{*}$. For the last elements in row, we have the following update:

$$\mathcal{B}(K, K) = 1 - \sum_{i=1}^{K-1} \mathcal{B}(K, 1 : K-1)$$

We compare the model parameter estimates with and without the assumption that B is symmetric in the simulation data. We assume π_k s are all the same across different blocks; the inter block connectivity $b = 0.05$, while the intra block connectivity $a = 1 - b * (K - 1)$. The K is set to be 3 and 5. The number of interactions are 1,500 and 2,500. The power-law parameter are set to be $\{\alpha_b\} = \{0.2, 0.5, 0.8\}$ and $\{\alpha_b\} = \{0.1, 0.3, 0.5, 0.7, 0.9\}$ correspondingly. We repeated 20 times for each setting. The mean value of the estimates for the diagonal elements of the propensity matrix for $K = 3$ and $K = 5$ are 0.902 (0.015) and 0.773 (0.066) correspondingly as compared to 0.899 (0.02) and 0.770 (0.069) with symmetry assumption and without symmetry assumption. The difference is almost negligible assuming \mathcal{B} is symmetric as compared to when \mathcal{B} is not.

A.10 Simulation results for varying θ s

In Section 4.0.2, we have shown the posteriors given $\theta_1 = \theta_2 = 5$. Though both $\{\alpha_b\}$ and $\{\theta_b\}$ are the power-law distribution parameters, the values of $\{\alpha_b\}$ have more contribution

1,000 interactions	Parameters	$\{\alpha_b\} = \{0.1, 0.9\}$	$\{\alpha_b\} = \{0.2, 0.8\}$	$\{\alpha_b\} = \{0.3, 0.7\}$	$\{\alpha_b\} = \{0.4, 0.6\}$
$\{a, b\} = \{0.9, 0.1\}$	α_1	0.378 (0.110)	0.360 (0.106)	0.451 (0.113)	0.495 (0.077)
	α_2	0.908 (0.015)	0.809 (0.023)	0.694 (0.069)	0.611 (0.057)
	Diagonal	0.910 (0.021)	0.910 (0.020)	0.906 (0.019)	0.902 (0.019)
$\{a, b\} = \{0.7, 0.3\}$	α_1	0.409 (0.206)	0.511 (0.167)	0.479 (0.102)	0.520 (0.096)
	α_2	0.863 (0.124)	0.748 (0.112)	0.705 (0.051)	0.593 (0.066)
	Diagonal	0.716 (0.030)	0.728 (0.031)	0.714 (0.031)	0.705 (0.032)
$\{a, b\} = \{0.5, 0.5\}$	α_1	0.736 (0.214)	0.677 (0.128)	0.619 (0.091)	0.567 (0.082)
	α_2	0.757 (0.172)	0.718 (0.115)	0.629 (0.084)	0.573 (0.081)
	Diagonal	0.540 (0.052)	0.541 (0.057)	0.554 (0.061)	0.535 (0.057)
10,000 interactions	Parameters	$\{\alpha_b\} = \{0.1, 0.9\}$	$\{\alpha_b\} = \{0.2, 0.8\}$	$\{\alpha_b\} = \{0.3, 0.7\}$	$\{\alpha_b\} = \{0.4, 0.6\}$
$\{a, b\} = \{0.9, 0.1\}$	α_1	0.225 (0.072)	0.289 (0.062)	0.364 (0.04)	0.443 (0.038)
	α_2	0.901 (0.006)	0.803 (0.009)	0.707 (0.013)	0.614 (0.02)
	Diagonal	0.901 (0.006)	0.901 (0.006)	0.902 (0.005)	0.901 (0.006)
$\{a, b\} = \{0.7, 0.3\}$	α_1	0.258 (0.092)	0.408 (0.161)	0.411 (0.11)	0.448 (0.056)
	α_2	0.902 (0.005)	0.785 (0.066)	0.695 (0.054)	0.603 (0.032)
	Diagonal	0.704 (0.009)	0.674 (0.068)	0.691 (0.044)	0.694 (0.035)
$\{a, b\} = \{0.5, 0.5\}$	α_1	0.865 (0.163)	0.724 (0.162)	0.626 (0.095)	0.549 (0.059)
	α_2	0.703 (0.127)	0.657 (0.126)	0.637 (0.081)	0.555 (0.051)
	Diagonal	0.51 (0.015)	0.51 (0.015)	0.513 (0.017)	0.51 (0.017)

Table 5: Posterior means (SD) of power-law parameters $\{\alpha_b\}$ and within/between cluster propensity $\{a, b\}$ in different settings, with $\{\theta_1, \theta_2\} = \{10, 10\}$

to the observed power-law properties. For the completeness, we show here the parameter estimates of the model parameters with varying values of θ s. to be more specific, we have θ s to be chosen from the following values: $\{\{10, 10\}, \{1, 1\}, \{10, 1\}, \{1, 10\}\}$. In all these settings, the conclusions based on the means of the posteriors are the similar to those when $\theta = \{5, 5\}$, with minor variations in the specific values.

A.11 Selection of K in settings with varying parameters

In Section 4.0.3, we briefly discuss a model selection criteria based on the maximal marginal likelihood. Figure 3 shows the likelihood as a function of K in other settings, where the propensity of within/between connections and the power-law parameters are different from

1,000 interactions	Parameters	$\{\alpha_b\} = \{0.1, 0.9\}$	$\{\alpha_b\} = \{0.2, 0.8\}$	$\{\alpha_b\} = \{0.3, 0.7\}$	$\{\alpha_b\} = \{0.4, 0.6\}$
$\{a, b\} = \{0.9, 0.1\}$	α_1	0.218 (0.157)	0.224 (0.140)	0.304 (0.141)	0.354 (0.142)
	α_2	0.898 (0.015)	0.796 (0.031)	0.681 (0.052)	0.585 (0.064)
	Diagonal	0.908 (0.016)	0.885 (0.014)	0.892 (0.057)	0.897 (0.019)
$\{a, b\} = \{0.7, 0.3\}$	α_1	0.367 (0.281)	0.276 (0.221)	0.374 (0.203)	0.341 (0.157)
	α_2	0.870 (0.100)	0.782 (0.100)	0.689 (0.074)	0.580 (0.079)
	Diagonal	0.667 (0.078)	0.691 (0.06)	0.678 (0.063)	0.694 (0.046)
$\{a, b\} = \{0.5, 0.5\}$	α_1	0.386 (0.268)	0.442 (0.266)	0.414 (0.237)	0.348 (0.186)
	α_2	0.900 (0.050)	0.753 (0.153)	0.623 (0.128)	0.526 (0.132)
	Diagonal	0.519 (0.033)	0.521 (0.037)	0.519 (0.037)	0.517 (0.033)
10,000 interactions	Parameters	$\{\alpha_b\} = \{0.1, 0.9\}$	$\{\alpha_b\} = \{0.2, 0.8\}$	$\{\alpha_b\} = \{0.3, 0.7\}$	$\{\alpha_b\} = \{0.4, 0.6\}$
$\{a, b\} = \{0.9, 0.1\}$	α_1	0.157 (0.111)	0.218 (0.121)	0.274 (0.101)	0.395 (0.075)
	α_2	0.900 (0.006)	0.803 (0.012)	0.691 (0.025)	0.591 (0.032)
	Diagonal	0.900 (0.006)	0.899 (0.005)	0.900 (0.005)	0.900 (0.006)
$\{a, b\} = \{0.7, 0.3\}$	α_1	0.378 (0.351)	0.216 (0.120)	0.268 (0.132)	0.354 (0.117)
	α_2	0.873 (0.067)	0.802 (0.012)	0.687 (0.031)	0.586 (0.050)
	Diagonal	0.653 (0.078)	0.693 (0.038)	0.660 (0.078)	0.680 (0.052)
$\{a, b\} = \{0.5, 0.5\}$	α_1	0.732 (0.262)	0.597 (0.259)	0.521 (0.199)	0.351 (0.191)
	α_2	0.853 (0.121)	0.721 (0.138)	0.672 (0.081)	0.567 (0.073)
	Diagonal	0.506 (0.011)	0.507 (0.012)	0.505 (0.011)	0.505 (0.010)

Table 6: Posterior means (SD) of power-law parameters $\{\alpha_b\}$ and within/between cluster propensity $\{a, b\}$ in different settings, with $\{\theta_1, \theta_2\} = \{1, 1\}$

1,000 interactions	Parameters	$\{\alpha_b\} = \{0.1, 0.9\}$	$\{\alpha_b\} = \{0.2, 0.8\}$	$\{\alpha_b\} = \{0.3, 0.7\}$	$\{\alpha_b\} = \{0.4, 0.6\}$
$\{a, b\} = \{0.9, 0.1\}$	α_1	0.212 (0.151)	0.297 (0.196)	0.354 (0.181)	0.384 (0.14)
	α_2	0.903 (0.016)	0.808 (0.038)	0.718 (0.054)	0.626 (0.049)
	Diagonal	0.900 (0.019)	0.887 (0.079)	0.885 (0.08)	0.899 (0.018)
$\{a, b\} = \{0.7, 0.3\}$	α_1	0.381 (0.312)	0.367 (0.232)	0.382 (0.201)	0.358 (0.152)
	α_2	0.895 (0.054)	0.781 (0.119)	0.704 (0.081)	0.633 (0.048)
	Diagonal	0.668 (0.079)	0.672 (0.074)	0.679 (0.065)	0.689 (0.05)
$\{a, b\} = \{0.5, 0.5\}$	α_1	0.548 (0.308)	0.502 (0.25)	0.568 (0.202)	0.5 (0.169)
	α_2	0.871 (0.122)	0.806 (0.076)	0.671 (0.119)	0.589 (0.101)
	Diagonal	0.513 (0.034)	0.526 (0.04)	0.518 (0.039)	0.525 (0.039)
10,000 interactions	Parameters	$\{\alpha_b\} = \{0.1, 0.9\}$	$\{\alpha_b\} = \{0.2, 0.8\}$	$\{\alpha_b\} = \{0.3, 0.7\}$	$\{\alpha_b\} = \{0.4, 0.6\}$
$\{a, b\} = \{0.9, 0.1\}$	α_1	0.143 (0.101)	0.186 (0.104)	0.31 (0.103)	0.396 (0.075)
	α_2	0.901 (0.006)	0.803 (0.011)	0.709 (0.013)	0.61 (0.018)
	Diagonal	0.899 (0.006)	0.900 (0.006)	0.900 (0.006)	0.899 (0.007)
$\{a, b\} = \{0.7, 0.3\}$	α_1	0.354 (0.319)	0.391 (0.262)	0.433 (0.195)	0.42 (0.113)
	α_2	0.900 (0.028)	0.794 (0.041)	0.694 (0.047)	0.609 (0.024)
	Diagonal	0.656 (0.081)	0.649 (0.081)	0.647 (0.075)	0.666 (0.069)
$\{a, b\} = \{0.5, 0.5\}$	α_1	0.751 (0.271)	0.629 (0.229)	0.596 (0.164)	0.531 (0.122)
	α_2	0.844 (0.109)	0.787 (0.06)	0.683 (0.08)	0.59 (0.063)
	Diagonal	0.506 (0.011)	0.508 (0.012)	0.506 (0.012)	0.508 (0.013)

Table 7: Posterior means (SD) of power-law parameters $\{\alpha_b\}$ and within/between cluster propensity $\{a, b\}$ in different settings, with $\{\theta_1, \theta_2\} = \{1, 10\}$

1,000 interactions	Parameters	$\{\alpha_b\} = \{0.1, 0.9\}$	$\{\alpha_b\} = \{0.2, 0.8\}$	$\{\alpha_b\} = \{0.3, 0.7\}$	$\{\alpha_b\} = \{0.4, 0.6\}$
$\{a, b\} = \{0.9, 0.1\}$	α_1	0.323 (0.099)	0.368 (0.091)	0.402 (0.064)	0.485 (0.078)
	α_2	0.893 (0.028)	0.789 (0.036)	0.691 (0.052)	0.582 (0.094)
	Diagonal	0.914 (0.02)	0.904 (0.02)	0.906 (0.019)	0.896 (0.022)
$\{a, b\} = \{0.7, 0.3\}$	α_1	0.369 (0.129)	0.459 (0.154)	0.46 (0.097)	0.477 (0.083)
	α_2	0.896 (0.024)	0.75 (0.099)	0.636 (0.101)	0.553 (0.097)
	Diagonal	0.702 (0.054)	0.714 (0.03)	0.711 (0.03)	0.701 (0.043)
$\{a, b\} = \{0.5, 0.5\}$	α_1	0.49 (0.222)	0.556 (0.19)	0.508 (0.157)	0.466 (0.142)
	α_2	0.859 (0.099)	0.665 (0.145)	0.576 (0.095)	0.546 (0.084)
	Diagonal	0.528 (0.044)	0.524 (0.048)	0.53 (0.047)	0.52 (0.045)
10,000 interactions	Parameters	$\{\alpha_b\} = \{0.1, 0.9\}$	$\{\alpha_b\} = \{0.2, 0.8\}$	$\{\alpha_b\} = \{0.3, 0.7\}$	$\{\alpha_b\} = \{0.4, 0.6\}$
$\{a, b\} = \{0.9, 0.1\}$	α_1	0.203 (0.067)	0.297 (0.056)	0.345 (0.042)	0.44 (0.03)
	α_2	0.900 (0.006)	0.798 (0.012)	0.697 (0.022)	0.586 (0.034)
	Diagonal	0.902 (0.006)	0.900 (0.007)	0.900 (0.007)	0.878 (0.085)
$\{a, b\} = \{0.7, 0.3\}$	α_1	0.286 (0.177)	0.302 (0.082)	0.343 (0.093)	0.442 (0.064)
	α_2	0.882 (0.082)	0.795 (0.018)	0.682 (0.041)	0.563 (0.056)
	Diagonal	0.692 (0.044)	0.686 (0.051)	0.668 (0.065)	0.639 (0.087)
$\{a, b\} = \{0.5, 0.5\}$	α_1	0.72 (0.265)	0.403 (0.181)	0.507 (0.156)	0.466 (0.094)
	α_2	0.726 (0.172)	0.776 (0.059)	0.603 (0.092)	0.531 (0.054)
	Diagonal	0.507 (0.012)	0.508 (0.012)	0.507 (0.013)	0.509 (0.013)

Table 8: Posterior means (SD) of power-law parameters $\{\alpha_b\}$ and within/between cluster propensity $\{a, b\}$ in different settings, with $\{\theta_1, \theta_2\} = \{10, 1\}$

the one shown in Section 4.0.3. The K that gives the MAP based on the empirical results is affected not only by the number of clusters in the generative model, but also by the strength of the connectivity and the power-law properties.

A.12 Likelihood pattern in TalkLife data

The averaged marginal likelihood over Gibbs iterations is shown in Figure 4. In the majority of sub-communities, the averaged marginal likelihood shows a monotonic pattern as function of the number of presumed blocks (Figure 4a). That is, the likelihood is the largest when $K = 2$ and keeps decreasing as K increases. There are several exceptions with the marginal likelihoods being maximized when K is greater than 2 (Figure 4c).

A.13 Case study with model fitting in other network

In Section 5.3, we showed two examples using Alcohol and Substance Abuse network and Behavioural Symptoms network. Note that not all the networks will give proper results due to the complexity of the underlying community structure. Here, we showed the results from fitting several more networks in Figure 5, including Body Imagining Eating Disorder Suspected network and Nssi Urge Suspected network. Our main conclusions remain the same as stated in the main context.

A.14 Fitting DC-SBM in the projected network

We show here the fitting results of the DC-SBM to the project Alcohol and Substance Abuse network. In the projected network, we say there exists an interaction between i and j only if the number of interactions between i and j reaches certain cutoff in the binary graph. We set the cutoff value to be 2. In the original binary graph, there are 30,744 edges. While in the projected network, there exist 4,218 edges, that accounts for only 13% of the interactions in the original network. Given the amount of the edges being trimmed, we didn't try the cutoff

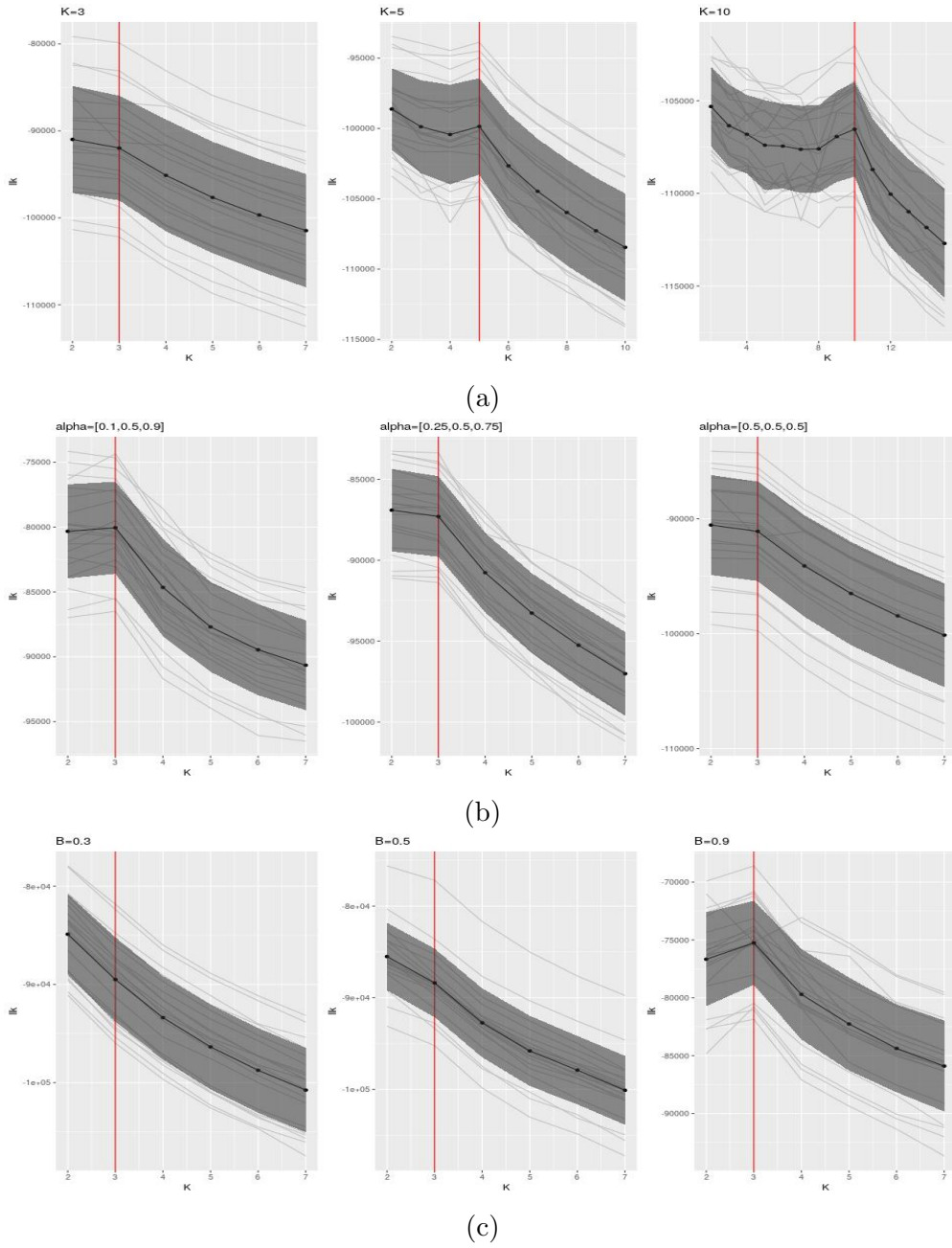


Figure 3: The trace plots of the likelihood in different settings. (a) For a varying choice of the underlying truth K , $a = 0.8$, $b = \frac{0.2}{(K-1)}$, $\alpha \sim \text{Uniform}(0.4, 0.8)$; (b) Fix $K=3$, $a = 0.8$, $b = 0.1$, $\{\alpha_1, \alpha_2, \alpha_3\} = \{\{0.1, 0.5, 0.9\}, \{0.25, 0.5, 0.75\}, \{0.5, 0.5, 0.5\}\}$; (c) Fix $K=3$, $\{\alpha_1, \alpha_2, \alpha_3\} = \{0.25, 0.5, 0.75\}$, $\{a, b\} = \{\{0.3, 0.35\}, \{0.5, 0.25\}, \{0.9, 0.05\}\}$

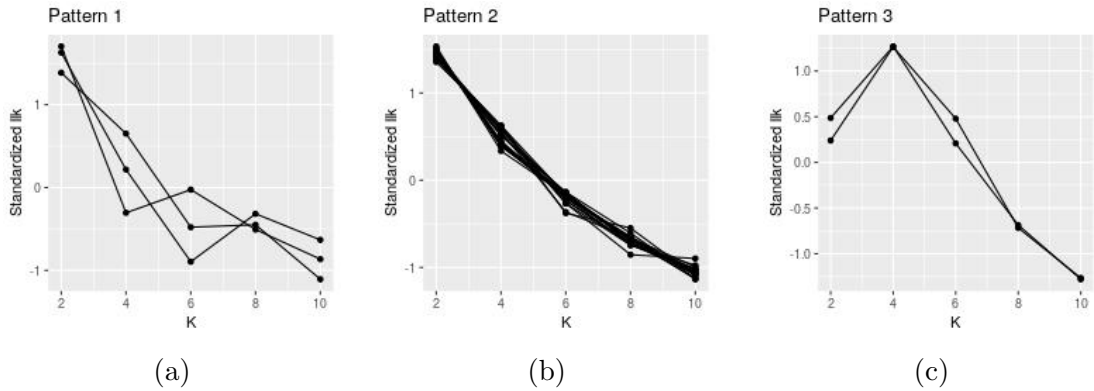


Figure 4: Different marginal log likelihood patterns observed in TalkLife networks. (a) The likelihood is maximized when $K=2$, but is not monotonic; (b) The likelihood is maximized when $K=2$, and is monotonic; (c) The likelihood is maximized when $K=4$. The log likelihoods in different networks are standardized to the same scale.

greater than 2. The results are shown in Figure 6 and Figure 7. The within block connections are more frequent in the projected network than before, but still weaker as compared to the other two methods. The HL distance is similar to what was observed before.

B Supplementary Materials

B.1 Supplementary Tables

B.2 Supplementary Figures

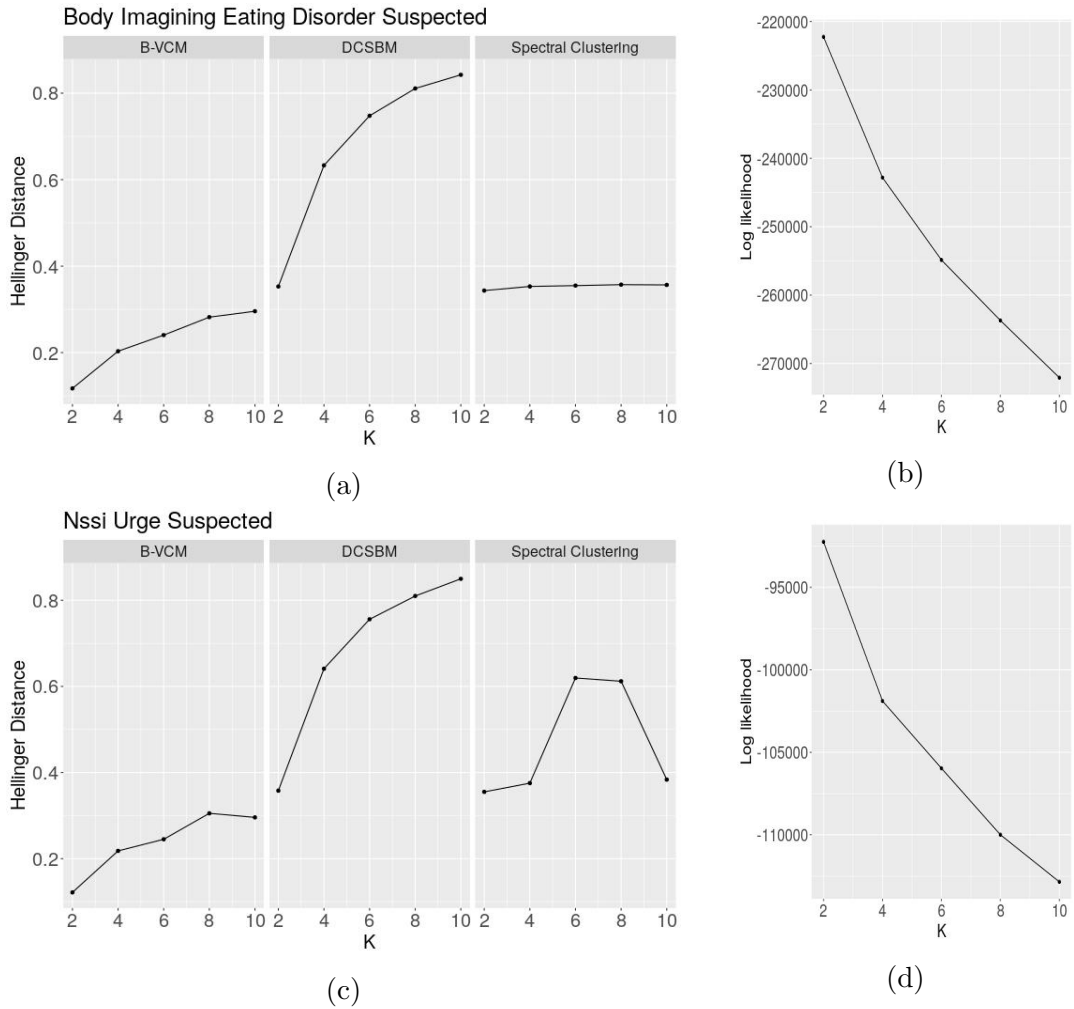


Figure 5: The Hellinger distances of the block assignment between the first half and the second half of the 2019 data in (a) Body Imagining and Eating Disorder network and (c) Nssi Urge network. The marginal likelihood over different K values in (b) Body Imagining and Eating Disorder network and (d) Nssi Urge network.

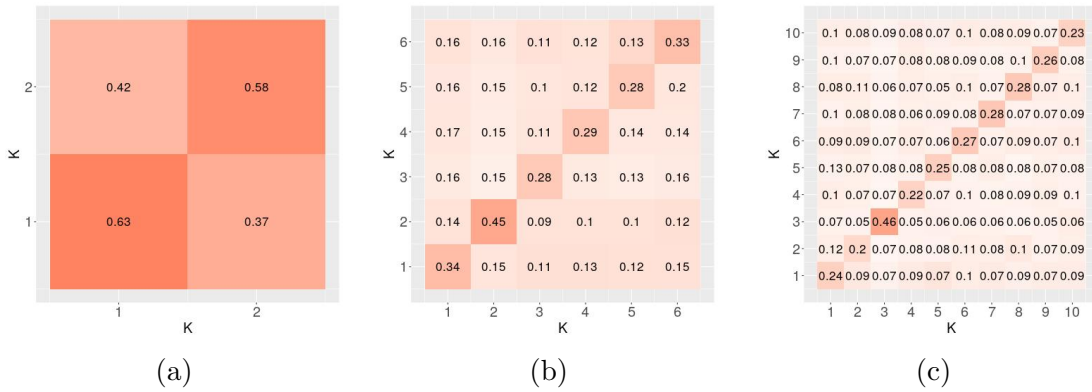


Figure 6: The inter/intra connectivity of the communities detected by DC-SBM in the projected network, ranging from 0 to 1, indicates the proportion of the interactions that initiated from one block to the other. The number within each cell is the proportion of the interactions initiated from one cluster (y-axis) to another (x-axis), normalized by each row.

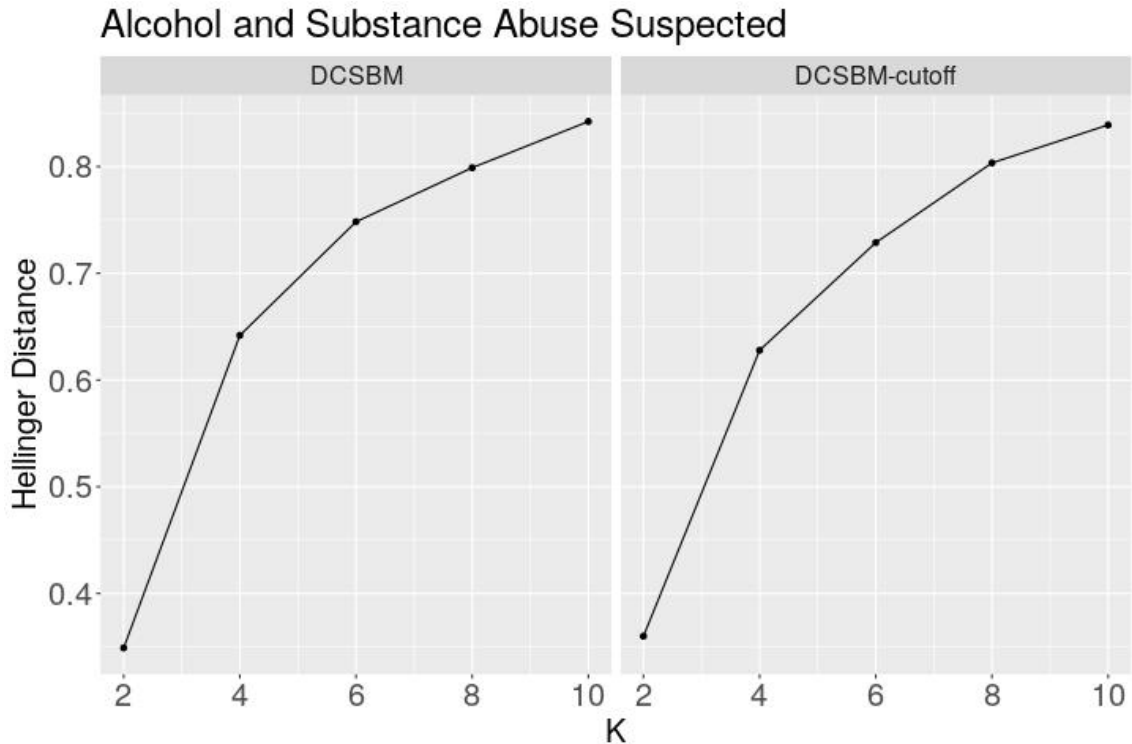


Figure 7: The Hellinger distances of the block assignment between the first half and the second half of the 2019 data in (a) Alcohol and Substance Abuse suspected network and (b) the projected network with the cutoff value being 2.

Tag names
AgitationOrIrritationSuspected
AlcoholAndSubstanceAbuseSuspected
AnxietyPanicFearSuspected
BehavioralSymptomsSuspected
BodyImageEatingDisordersSuspected
CryingSuspected
DeathOfOtherSuspected
DepressedMoodSuspected
DistortedThinkingSuspected
EmotionalExhaustionSuspected
EmptinessSuspected
FailureSuspected
FamilyIssuesSuspected
FinalTiredFatiguedLowEnergySuspected
HelplessnessHopelessnessSuspected
InpatientOutPatientMedicationSuspected
LonelinessSuspected
MentalHealthTreatmentSuspected
NauseaSuspected
NauseaWithEatingDisorderSuspected
NssiIdeationAndBehaviorSuspected
NssiUrgeSuspected
NumbnessEmptinessSuspected
NumbnessSuspected
SelfHarmRelapseSuspected
SelfHarmRemissionOrRelapseSuspected
SelfHarmRemissionSuspected
SelfHarmSuspectedTakeTwo
SongLyricsSuspected
SuicidalIdeationAndBehaviorSuspected
SuicidalPlanningSuspected
SuicideAttemptSuspected
TiredFatiguedLowEnergySuspected

Table 9: Name of all the Tags in the TalkLife data



Figure 8: The trace plots of the Gibbs samplers of α_1 and α_2 . Each row corresponds to different underlying α values, marked in the solid line; each column corresponds to different $\{a, b\}$, which takes the value from $\{0.1, 0.9\}$, $\{0.3, 0.7\}$, and $\{0.5, 0.5\}$

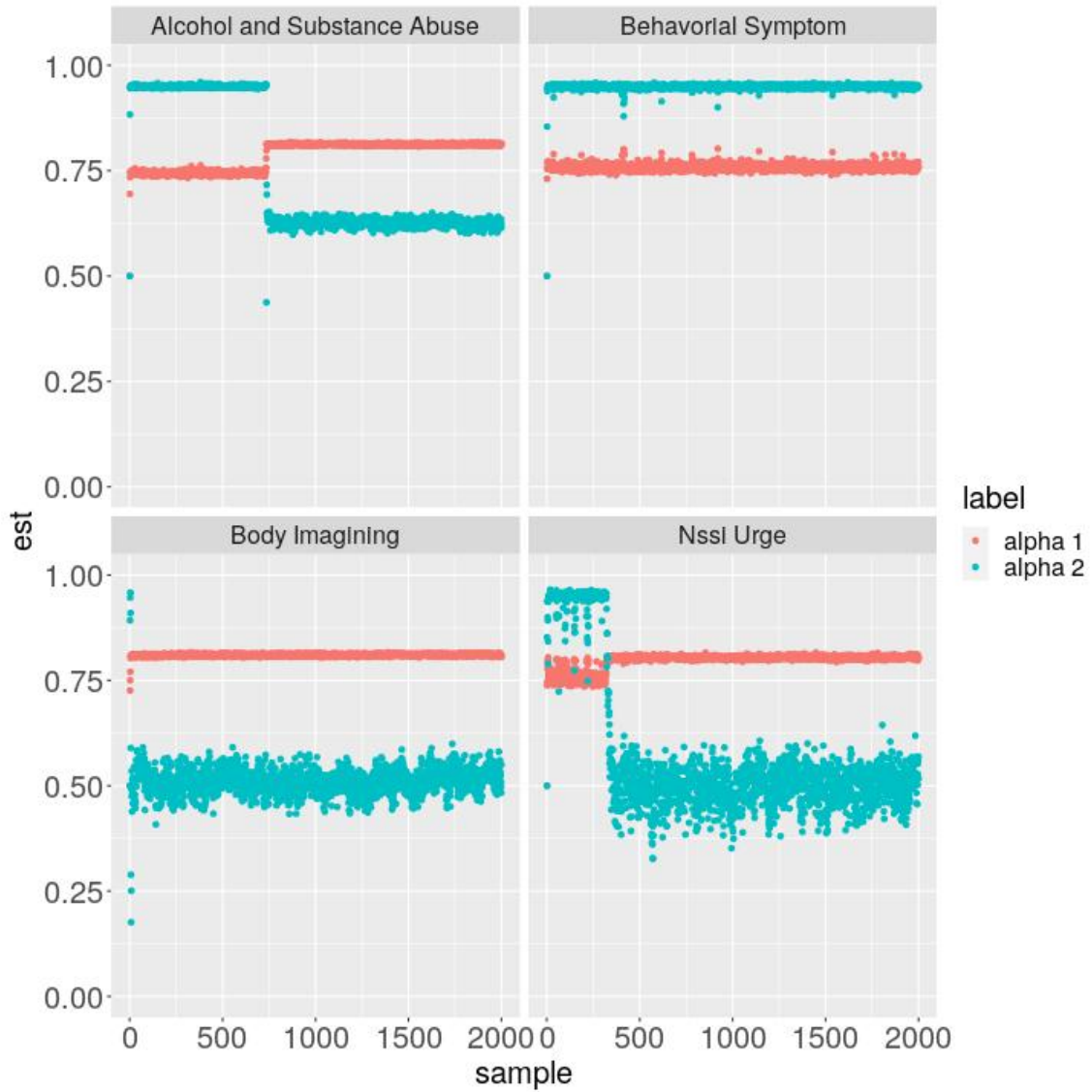


Figure 9: The trace plots of the Gibbs Samplers in different sub networks in TalkLife data, when setting the number of blocks to be 2.

C Code to Replicate Simulation and Case Study Results

The R code used to generate the simulation experiments and case study results in this paper can be obtained at <https://github.com/YuhuaZhang1995/B-VCM>.